GEOLOGY OF THE TEKMAN (ERZURUM) BASIN AND PETROLEUM POSSIBILITIES

Abdullah GEDİK*

ABSTRACT.— In the investigated area, Paleozoic aged Akdağ metamorphics, Cretaceous aged Şahvelet ophiolitic complex, Upper Cretaceous aged Derviş Halit formation, Eocene aged Musakomu and Gımgımtepe formations, Oligocene aged Ağcakoca formation, Miocene aged Hürübaba, Haneşdüzü and Hacıömer formations, Pliocene aged İncesu formation, Middle Miocene aged Aras volcanics and Plio-Quaternary aged Yıldırımdağ basalts are exposed. Katranlı stream area active oil seepages are present. ,Mesozoic-Tertiary aged formations have intervals having the characteristics of source rocks, reservoir rocks and cap rocks.

PALEOSTRESS TRAJECTORIES AND POLYPHASE RIFTING IN ARC-BACKARC OF EASTERN PONTIDES

Osman BEKTAŞ*

ABSTRACT.— In the modern convergent plate margins geological and geophysical evidences imply that maximum horizontal stresses (sHmax) over the overriding plate are transmitted from plate boundry to the backarc region. This causes compressive regime in the plate boundry and extensive regime in the backarc or inner part of overriding plate. Depending on the age and properties of downgoing plate and relative motion of the overriding plate maximum compressive stresses (s) are transmitted as s2 (sl> s2> s3) in the consuming direction or parallel to the arc from trench zone to backarc region. Though strike slip motions are dominant in the arc, they are associated to extensional and compressional regions. Geological data from Eastern Pontides, especially southern part of arc seem to show that tecto- nics is predominantly extensional and   several   short lived compressional phases break up this extentional regime during Mesozoic same as in the Agean and Japan arcs. First extensional regime started in Lias or Pre-Lias and ended in Malm-Late Lower Cretaceous. In this period many ensialic intra-arcbasins to the   north and   ensimatic backarc basins with axial through sea floor spreading (Malm-Lower Cretaceous ophiolite) to the south had been developed (Mariana type subduction). Short lived compressional phase between Late Lower Cretaceous and Early Upper Cretaceous detracted these basins (Chilean type subduction). Under a new extensional regime Eastern Pontian are and backarc rifted again and new axial sea floor spreading occurred to the south to form Upper Cretaceous ophiolites. The formation of Krukko type polymetalic ore deposits along the Black Sea coast correspond to this stage (intra-arc rifting). Intra- arc and backarc basins closed again by following compressive stresses between Late Upper Cretaceous and Early Eocene. Except for sea floor spreading polyphase rifting should have been in the same way during Cenozoic time. In addition to diverse folding axes and opposite direction thrusting may imply that strike slip motion may be associated to compressional and extensional regime in Eastern Pontides. As a result except very short lived compressive stresses southern part of Pontides is the extensional region or extensive stresses increase from north to south. Such a result indicates that southern part of Pontides was the backarc region and it is in favor of southward subduction during Meso- zoic and Cenozoic time.

INTRODUCTION

In the modern convergent plate margins geophysical (solutions of earthquake epicentral mech- anisms) and geological evidence brings up important results about changes of maximum horizontal tectonic stresses over the overriding plate. It is obvious that intra-plate horizontal stresses cause different geological events depending on their characteristics. From this point of view, geological events in paleotectonic environments or in ancient consumption zone can give explanatory information about maximum horizontal stresses that have occurred in the past.

Several authors have used different methods for interpretation of the evolution of Eastern Pontides obtaining different results (Dewey et al., 1973; Adamia et at, 1977; Şengör et at, 1980; Tokel, 1981; Bektaş, 1981, 1982, 1983; Bektaş et at, 1984). The purpose of this paper is to make clear what type of horizontal stresses were required for the geological characteristics of Eastern Pontides gained during Mesozoic and Cenozoic (distribution of magmatic provinces along Pontian arc, facies analyses, structural elements, the position and geotectonic significance of the ophiolitic belt south of the arc, etc.) and to correlate the obtained results together with the data taken from the modern consuming zones. The conclusions reached so far, from a different point of view, will lead to limitation of the interpretations above to a narrowed field.

STRESS DISTRIBUTION IN CONVERGENT PLATE MARGINS

Uyeda and Kanamori (1979), Nakamura and Uyeda (1980), Uyeda (1983) have derived and generalized, in time and space, the variations of stress distributions in Alaska-Aleutian, Middle Europe, Agean arc, southwestern and northeastern Japanese arc and back-arc regions (Fig. 1).
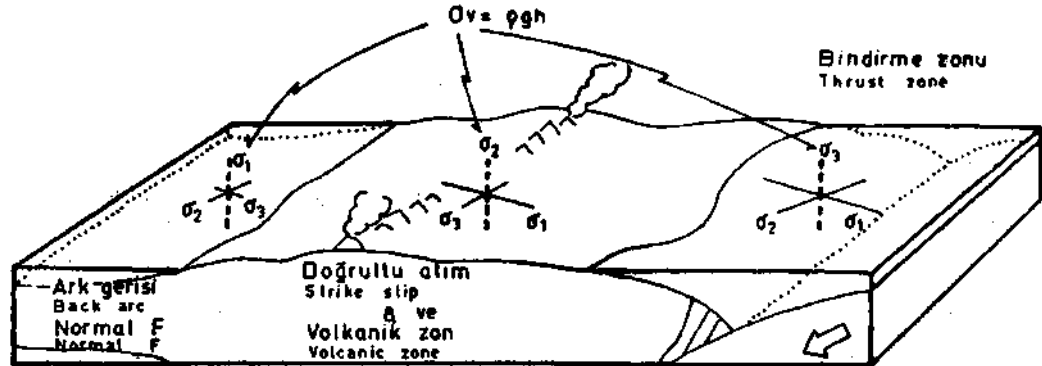

Fig. 1 - Schematic drawing showing a typical case where σ Hmax decreases from the trench toward the backarc region across the volcanic arc. Here σl> σ2> σ3 (Nakamura and Uyeda, 1980).

On the trench side of arcs (Front zone of convergence) the intensity of the dominant   compressive stresses varies with the age of the subducting oceanic plate, the characteristics of plate interaction zones, the progressive and reprogressive role of the overriding plate and the position of the trench. Because of the unrigid behaviour of the overriding plate the compressional stresses can not be transmitted to the inner parts of the plate. Therefore the maximum horizontal stresses (sHmax) decrease towards the inner parts. When sHmax <sV (vertical stress), horizontal compressive stresses transform from s1 to s2 (s1>s2>s3) .sl generally does not transform to a2 in the consumption direction. In the backarc region, a2 changes its strike and takes a parallel attitude to the arc because of the gravitational forces and shear stresses over downgoing lithosphere caused by convection currents in the mantle. This period   corresponds to backarc and intra-arc normal and strike-slip faulting (rifting) or backarc   sea floor spreading (Mariana type of consumption or period of minimum interplate stresses). The period in which sl is transmitted to the backarc is defined by folding, reverse and strike-slip faulting in the intra-arc and backarc regions (Chilean type of consumption or the period of maximum inter-plate stresses).

As a summary it can be said that in convergent plate boundaries, compressional stresses are dominant in fore arc and extensional stresses in backarc regions. The arc is located between compressed and tensioned regions. In other words, horizontal stresses are of the intermediate type. When the backarc sea floor spreading is possible rifting is generally parallel to the arc. This shows the transmission of sHmax(s2) from consumption direction to a parallel position to the arc. Figure 2 shows the intensity and strike variation models of sHmax stresses in the arc and backarc regions. In the first position, sHmax is transmitted from sl to s2 in the consumption direction (rifting in consuming direction in the backarc; Middle America and Middle Europe). In the third position, sl, in the consuming direction, is transmitted to s2 in backarc (backarc rifting and sea floor spreading; Japanese arc in Miocene, Aleutian arc, West Greece and Albania). The second position is the transition between first and third positions (Agean arc, West Japan, Alaska continent).

Extensional stresses are dominant in the Agean Basin. Extensional stresses of long durations alternated with tectonic phases of Upper Miocene-Lower Pliocene and of Lower Pliocene age (Mercier, 1981). The same is valid for the Japanese arc (Uyeda, 1983). Mercier (1981) analysed the compressional and extensional stresses of the active plate margins such as the Agean arc and the Andes. He pointed out that, in the plate over the consumption zone, most of the deformations caused by compressional stresses are related to the extensional conditions of convergent plate margins. On the other hand, sysmotectonic works show that extensional stresses in the Andaman backarc basin and compressional stresses in the overriding plate of Burma are dominant (Mukhopadhyay, 1984).
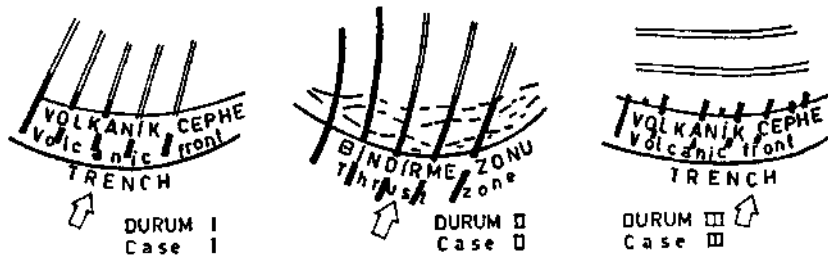

Fig. 2 - Schematic diagrams showing different patterns of the horizontal tectonic stress (σHmax) trajectories in arc and backarc regions. Case II is the transition between cases I and III. σHmax is represented by dark lines where it refers to σ1 and by lighter ones where it refers to σ2 (Nakamura and Uyeda, 1980).

EXTENSIONAL-COMPRESSIONAL STRESS PERIODS IN ARC-BACKARC OF EASTERN PONTIDES

In the Eastern Pontian arc, same as with any other active plate margin, extensional stress periods of long durations (rifting and sea floor spreading) alternated with short periods of compressional stress resulting in folding, reverse faulting and complete or partial closure of basins. So as it is mentioned above, many sedimentary basins have been formed and closed alternatively due to subduction mechanism in the arc and backarc of Eastern Pontides during Mesozoic and Cenozoic (polyphase rifting). On looking at the geological events as a whole, it can be concluded that especially the southern part of the Pontian arc is generally an extensional area or according to the explanations above a back-arc geotectonic environment is present. The extensional periods in the stress regimes of Eastern Pontides are distributed as follows:

Liassic-Lower Cretaceous

Sedimentologic, tectonic and geomorphologic evidences show that there was an extensional regime in the region during this period (Pelin, 1977; Eren, 1983; Görür et al., 1983; Bektaş et al., 1984). Liassic formations were deposited in E-W trending grabens in the south and parallel to the arc. These grabens were bounded by horsts (Gümüşhane granite, Köse granite, Pulur Massif and Kop serpentinites). These volcano-sedimentary sequences show changes in thicknesses and facies in a restricted area. The volcano-sedimentary Liassic unit generally contains coarse and fine elastics, ammonite bearing red limestones, basaltic dykes, sills and lavas. This unit unconformably overlies an ancient continental unit (metamorphic or granites of Paleozoic age) around Yusufeli-İspir,

Gümüşhane, Bayburt, Reşadiye, Niksar and Havza: The same rock units overlie the serpentinites around Kop and Demirözü in the south. However no serpentinite fragments were found in the basal conglomerates. Transition from a sialic basement in the south to a simatic crust in the north can imply argumentation of intra-lithospheric extensional stress from north to south causing a crustal and lithospheric shortening (McKenzie, 1978; Cochron, 1983). From this point of view, it can be thought that the Kop and Demirözü peridotites and gabbros are the diapirs (ophiolites due to rifting) intruded in the continental crust before the sea floor spreading during the backarc rifting of Eastern Pontides (Bektaş et al., 1984). The basalts of the volcano-sedimentary unit metamorphosed in green schist facies and Malm-Lower Cretaceous in age are associated with peridotites around Erzincan and characterize a mid-oceanic subduction zone (Bektaş, 1981). This evidence indicates a stronger extensional regime for the later period of the rifting and implies sea floor spreading along the rift axes south of the arc. As a summary, the backarc basin of Eastern Pontides during Malm-Lower Cretaceous was similar to that of the modern Red Sea. The deep marine sediments (pelagic carbonates, radiolarites, turbidites and olistostroms) of Malm-Lower Cretaceous age around Bayburt, Maden and Otlukbeli refer to the maturing period of the rifted backarc basin. The geological evidences outlined above imply an extensional regime in the region from Pre-Liassic or Liassic up to the Late Lower Cretaceous resulting in rifting and formation of sedimentary basins.

Upper Cretaceous-Paleocene

An extensional period was followed by a short compressional period during Late Lower Cretaceous or Early Upper Cretaceous. Hence, Lower Cretaceous sediments were folded, uplifted and faulted. The effects of this orogenic phase are well known throughout the Pontides (Ketin, 1962; Gattinger, 1962; Pelin, 1977; Terlemez and Yılmaz, 1979; Gedikoğlu et al., 1979; Akyürek et al., 1984). In contradiction to the view of Terlemez and Yılmaz (1979), Seymen (1975) reported a graditional relation between Lower Cretaceous and Upper Cretaceous. This orogenic phase was active throughout the Pontid Belt and it is well known in the Alpine Belt. But according to the evidences above, there may be some inner basins preserved during this period or a phase might have occurred during the closure of basins (Lower-Upper Cretaceous gradation).

The development of backarc and intra-arc basins parallel to the Pontian arc shows the effects of a new extensional period from Cenomanian-Turonian onwards. Facies changes of the same age (turbidites, pelagic red limestones and reefal limestones) bounded by intra-basin faults are indicative of horst-graben structures. The Upper Cretaceous sediments are represented by basal conglomerates followed by Nerinia bearing sandy limestones. Distal turbidites and volcanics interbedded with these turbidites belong to the uppermost section of the Upper Cretaceous. (Seymen 1975; Pelin, 1977; Turan, 1978; Eren, 1983; Hacıalioğlu, 1983; Bektaş, 1985). The Upper Cretaceous also starts with a basal conglomerate and continues with a volcano-sedimentary unit around Harşit Valley (Gedikoğlu et al., 1979) and Artvin (Van, in print). The lithofacies changes, the characteristics of the volcanism and the geotectonic setting of the north and south zones of Eastern Pontides are described in details (Bektaş, 1984). The extensional stresses are more continoues and intense in south zones and the lithosphere is sufficiently thin (Cochran, 1983; Turcatte, 1983) in axial areas of rifts to cause ocean floor spreading during Upper Cretaceous (the ophiolitic belt of Erzincan-Sivas-Ankara; Bektaş, 1983). During this period, similar and restricted rifting resulted in formation of intra-arc basins in which a tholeitic-calc alkaline volcanism and associated polymetalic ore deposition were formed. In other words, during Upper Cretaceous we see a tholeitic-calc alkaline volcanism and the formation of ensialic intra-arc basins in the north and a calc alkaline-alkaline volcanism and the formation of backarc ensialic-ensamatic basins in the south just as it was during Jurassic. Back-arc

rifting and related ocean floor spreading is reflected as ophiolites and accompanied tholeitic-calc alkaline volcanism (Bektaş, 1981) in the south.

Eocene

The backarc and intra-arc basins of the Upper Cretaceous in the Eastern Pontides closed in the Late Paleocene and therefore a compressional regime has started in the region and a new erogenic phase developed. The Eocene sediments, unconformable on the basement, are represented by distal flysch or shallow marine and lagoonal sediments. This geologic setting corresponds to the Eocene volcanism and contemporaneous rifting. However, the horizontal extensional stresses were not continous and intense as they were in the Upper Cretaceous and ocean floor spreading is unlikely. Eocene volcanism is of calc alkaline-alkaline affinity in the south (Terzioğlu, 1984) and calc alkaline in the north of Eastern Pontides (Eğin and Hirst, 1979). This reveals that the southern zone was in backarc tectonic setting during this period, too. Geological setting shows that such extensional and compressional periods were alternating during Cenozoic. But, this subject will not be discussed in detail, here.

POLYPHASE RIFTING IN SPECIFIC DIRECTIONS

As stated above, polyphase rifting occurred in Eastern Pontides during Mesozoic and Cenozoic. Geological evidence suggests rifting in Liassic exclusively occuring along the Pontides (Schultze-Westrum, 1961; Nebert, 1961; Seymen, 1975; Pelin, 1977; Saner, 1980; Öztürk, 1980; Görür et al., 1983). Using the geological and geophysical evidence, rifting in the Eastern Pontides during Upper Cretaceous is suggested by Bektaş (1984) and west of Çankırı-Çorum basin by Akyürek et al. (1984) and Ünalan and Yüksel (1978). Both of the rifting occurred in the same regions and directions parallel to the arc and ophiolitic belt. At least three marginal basins were opened and closed successively on the Anatolian ophiolitic belt which was an ancient suture zone during Triassic, Jurassic-Cretaceous and Upper Cretaceous. But in the Eastern Pontides, the existance of an oceanic domain during Triassic is not supported by sufficient evidence. In other words, the ancient rifting or suture zones are preferable areas for development of rifts and ocean floor spreading.

Vink et al. (1984) claims that continental crusts are three times weaker than the oceanic ones and they indicate that the preferable rifting occurs along ancient rifts and suture zones; also emphasizing the reliability of the idea by quoting from Wilson (1968) «Immature ocean floors develop on the suture zones of the previously closed oceans». It is known that, due to the subduction of Pasific plate under the Eurasian, the extensional periods on the China continental shelf caused polyphase rifting (Desheng, 1984). These petroliferous intra-plate rift basins which are supposed to develop in relation to the rising mantle diapirs on the consumption zones, seperated by geanticlines. According to various investigations carried out in the Alpine Belt, basins smaller than the Atlantic Ocean may be closed in a very short time (Zwart and Dornsiepen, 1978; Trümpy, 1981). It is claimed that the Alpine ocean was closed within 100 m.y. in the medial Alps (Frisch, 1979) and in 50 m.y. in the Southern Alps (Winterer and Bosellini, 1981). On the other hand, Le Blanc (1981) proposed smaller basins rather than the Atlantic type for the Pan-African and Tethyan ophiolites. Similar to this, Moores etal., (1984) concluded that all the ophiolitic rocks of the Middle East from Cyprus to Omman are related to the backarc basins and their ocean floor spreading developed on the oblique consumption zones like the Andaman Sea. It can be outlined that the Middle Anatolian ophiolitic belt contains fragments of oceanic crust generated by polyphase rifting during Mesozoic. The basins are closed completely or partially during orogenic phases.

PALEOSTRESS DISTRIBUTION IN EASTERN PONTIDES

The setting, type, intensity and variations of the paleostress distributions of the convergent plate margins, in time and space, are derrived from the mechanical meaning of some elements such as dykes, folding and faulting in the region (Zoback, 1980; Nakamura and Uyeda, 1980; Engelder

and Geiser, 1980). Kronberg (1969) and Yıldız (1984) have studied the fault tectonics of the Eastern Black Sea range by photogeological means concluding 50° and 130° striking fault systems were active since the Lower Jurassic. When the dyke and fold systems of Mesozoic and Cenozoic age in the Eastern Pontides are analysed one can observe perpendicular (orthogonal) fold and dyke systems similar to that obtained by Kronberg. On considering the parallel nature of sedimentary and rift basins parallel to the arcs, one can observe that extensional and compressional stresses were active successively or were contemporaneously in a similar fashion during Mesozoic and Cenozoic. Therefore compressional and extensional periods in the region-and their causes must be evaluated seperately. Any period of compressional stress also shows variations in itself. The dominant ENE-WSW striking fold axes and reverse faults of Eastern Pontides must have been developed by the maximum horizontal compressional stresses produced by al, active in the NNW-SSE direction. The setting of this compressional stress is defined by the dykes having the same strikes (Fig. 3). In spite of this, folds striking ambigously WNW-ESE are the result of maximum compressional stress (s) defined by NNE-SSW striking dykes (Fig. 4). As stated previously, the horizontal maximum compressional stresses (sl) in arc and backarc regions cause compressional stresses in the direction of consumption. Thus, the presence of (sl) in two different directions during the compressional stress period in the Eastern Pontian arc reveals the following possibilities:

1. Such a great change (90°) in the direction of maximum horizontal compressional stresses can be explained either by the rotation of al by 90 degrees or by the relative replacement of s1 and s2 (relative decreasing and increasing of their intensities). A modern example to this is Northwest Pacific region in the North America, al should be active in the direction of consumption and is parallel to the arc due to strike slip faulting (Zoback and Zoback, 1980). If sl directions in the Eastern Pontides are represented by the maximum compressional stresses in the consumption direction and produced by the friction between subducting and obducting plates, it can be concluded that the active margin should be affected by the complex relative plate movements as it is in the Middle America (Kellog and Bonini, 1982).

2. It is possible to consider stresses as right lateral and left lateral couples, perpendicular to fold axes, in the directions of NE-SW and NW-SE instead of evaluating stresses (s1) in various directions as maximum horizontal stresses. This opinion can explain the presence of fold and dyke systems (orthogonal system) perpendicular to each other developed successively and/or contemporeneously and supports Kronberg's (1970) theory. That is the modern Eastern Pontid joint system (50-130) is parallel to the strike slip faulting during Mesozoic and Cenozoic. If the second view which seems plausible on consideration of the geotectonic structure of the region, is accepted it can be concluded that maximum horizontal compressional stresses have worked in N-S and in the direction of consumption and caused strike slip faulting in arc and backarc regions. The periods of development of intra-arc and backarc basins and backarc ocean floor spreading in south of the arc (horizontal stresses < vertical stresses) correspond to the time when horizontal maximum compressional stresses were (s2) in E-W direction (Fig. 5). Normal faults, horsts and grabens parallel to these and dykes of the same direction are the main geotectonic elements of the extensional stress regime. During an extensional stress period the maximum compressional stress al should be transformed to s2 from N-S to E-W direction and during this period a2 is horizontal and parallel to the normal fault strike, s3 is horizontal trending N-S and al is vertical. But where maximum (al) and intermediate (s2) compressional stresses replace each other in time, strike slip faulting should develop in intra-arc and backarc basins. This is balanced by the reversal of strike slip faulting during compressional stress regimes.

As a summary, the N-S directed maximum compressional stresses (sl) have caused closure of previous basins, folding of the basement rocks and sediments and uplift by reverse faults and the extensional stresses of the same direction have caused formation of new sedimentary basins and new ocean floor spreadings in the Eastern Pontides during Mesozoic and Cenozoic (Fig. 6 and 7). During these two different tectonic regimes, strike slip faulting must have occurred when s2 replaced s3 in compressional stress periods and s1 replaced s2 in extensional stress periods. Modern two linament systems are the inheritors of the ancient linament systems.
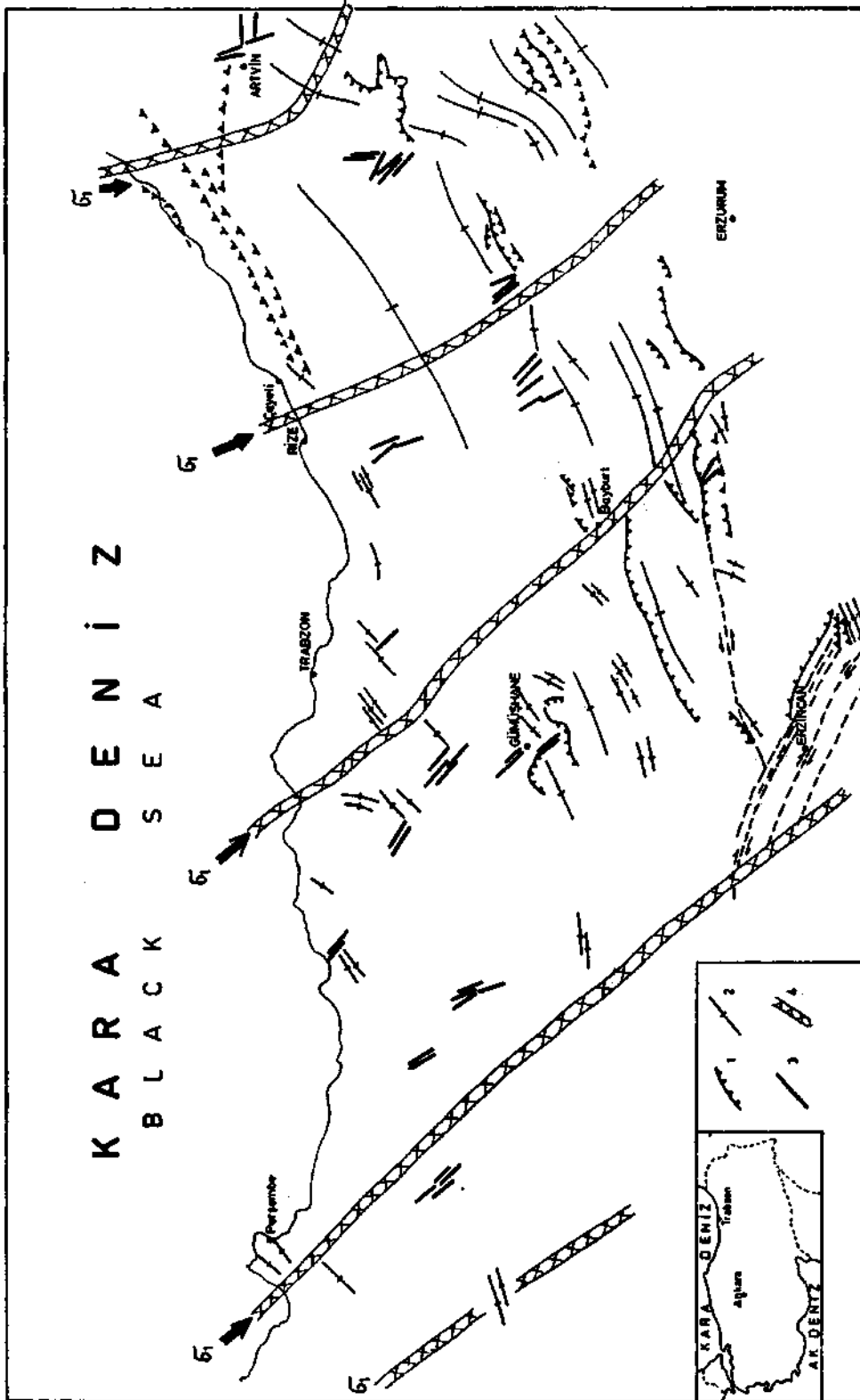
Fig. 3 – The maximum compressional stress periods in the Eastern Pontides during Mesozoic and Cenozoic; the setting of related dominant dykes, fold axes and thrusts. 1 – Thrust fault; 2 – Fold axis; 3 – Dyke; 4 – σ1, the direction of maximum compressional stress in the compressional regime.
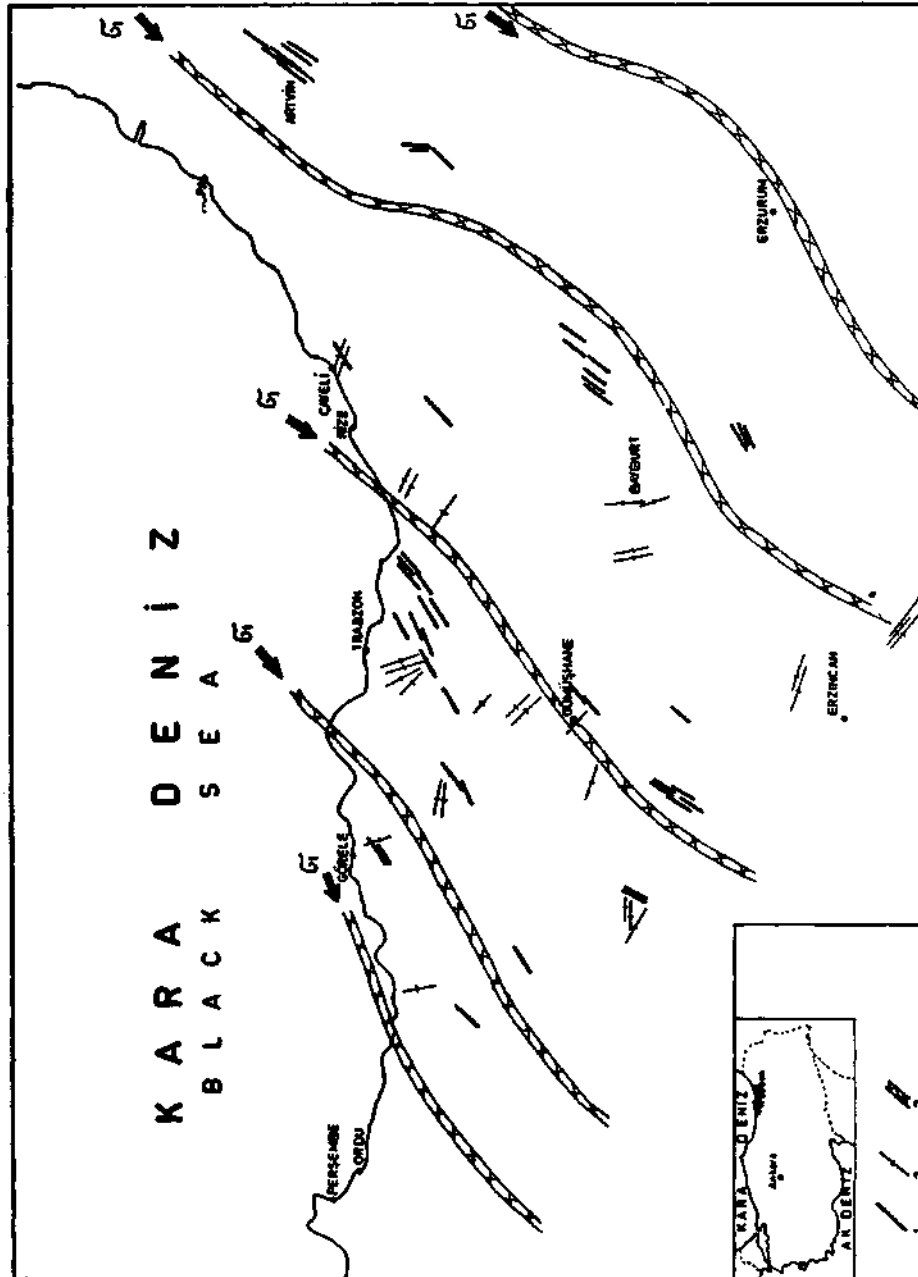
Fig. 4 - The maximum compressional stresses in the Eastern Pontides during Mesozoic and Cenozoic; the position of related less apparent dykes and fold axes.

1 - Dyke; 2 - Fold axis; 3 - The direction of maximum compressional stress ($\sigma 1$).
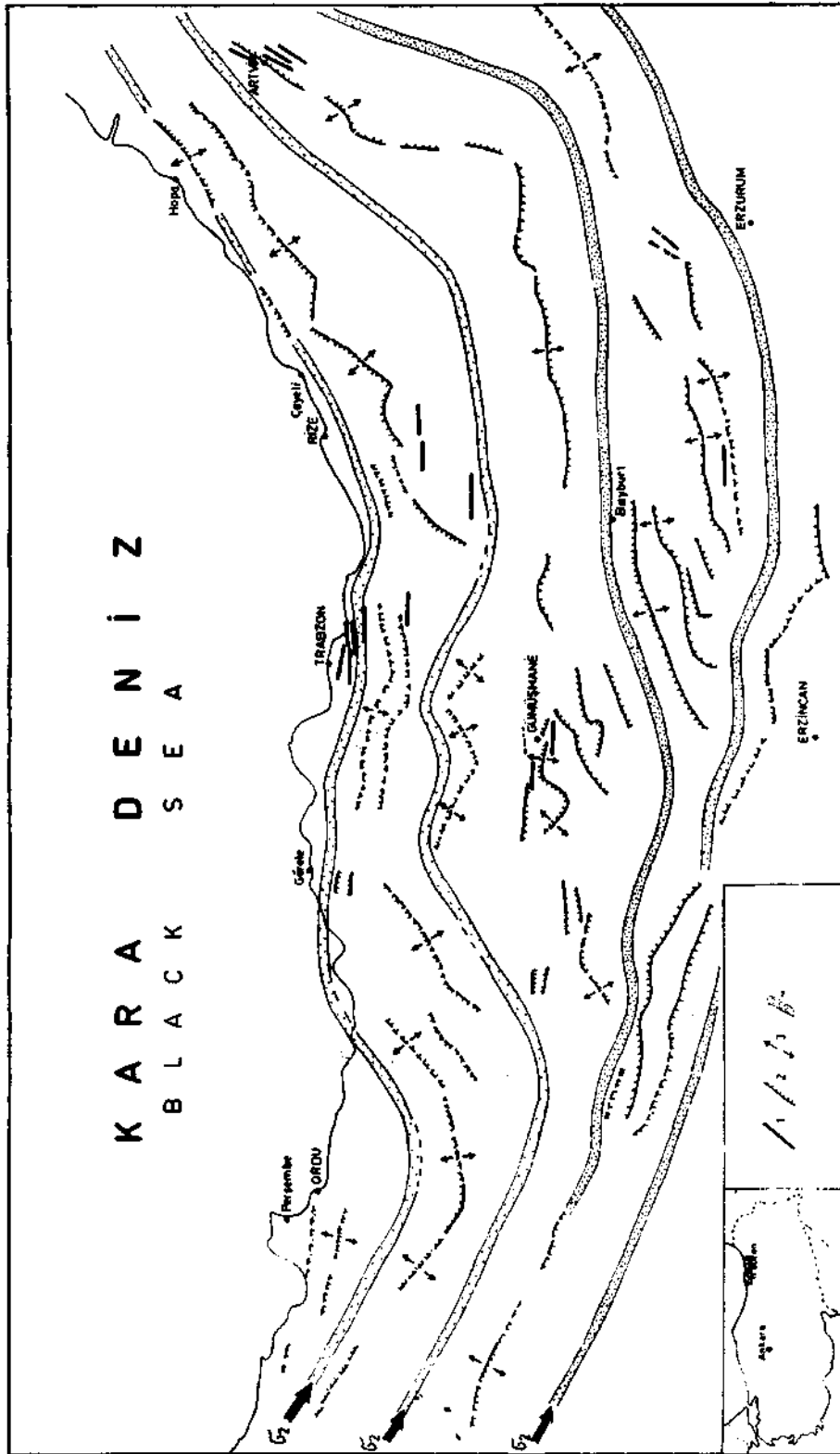
Fig. 5 - The maximum compressional stress in the Eastern Pontides during the extensional regimes of Mesozoic and Cenozoic; related dykes, normal faults and rift direction. 1 - Dyke; 2 - Normal fault associated to rifting; 3 - Extension direction; 4 - Maximum compressional stress ($\sigma 2$).

Fig. 6 - The geotectonic model corresponding to the orogenic periods in the Eastern Pontides.

Fig. 7 – The geotectonic model corresponding to the extensional periods in the Eastern Pontides.

DISCUSSION AND CONCLUSIONS

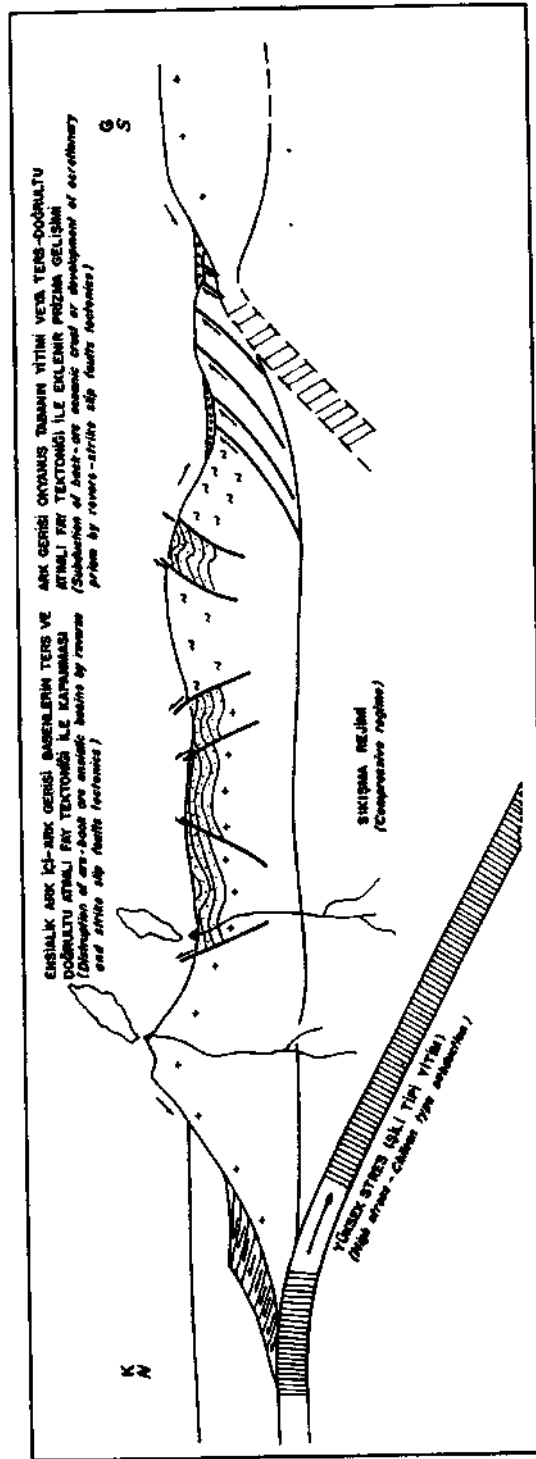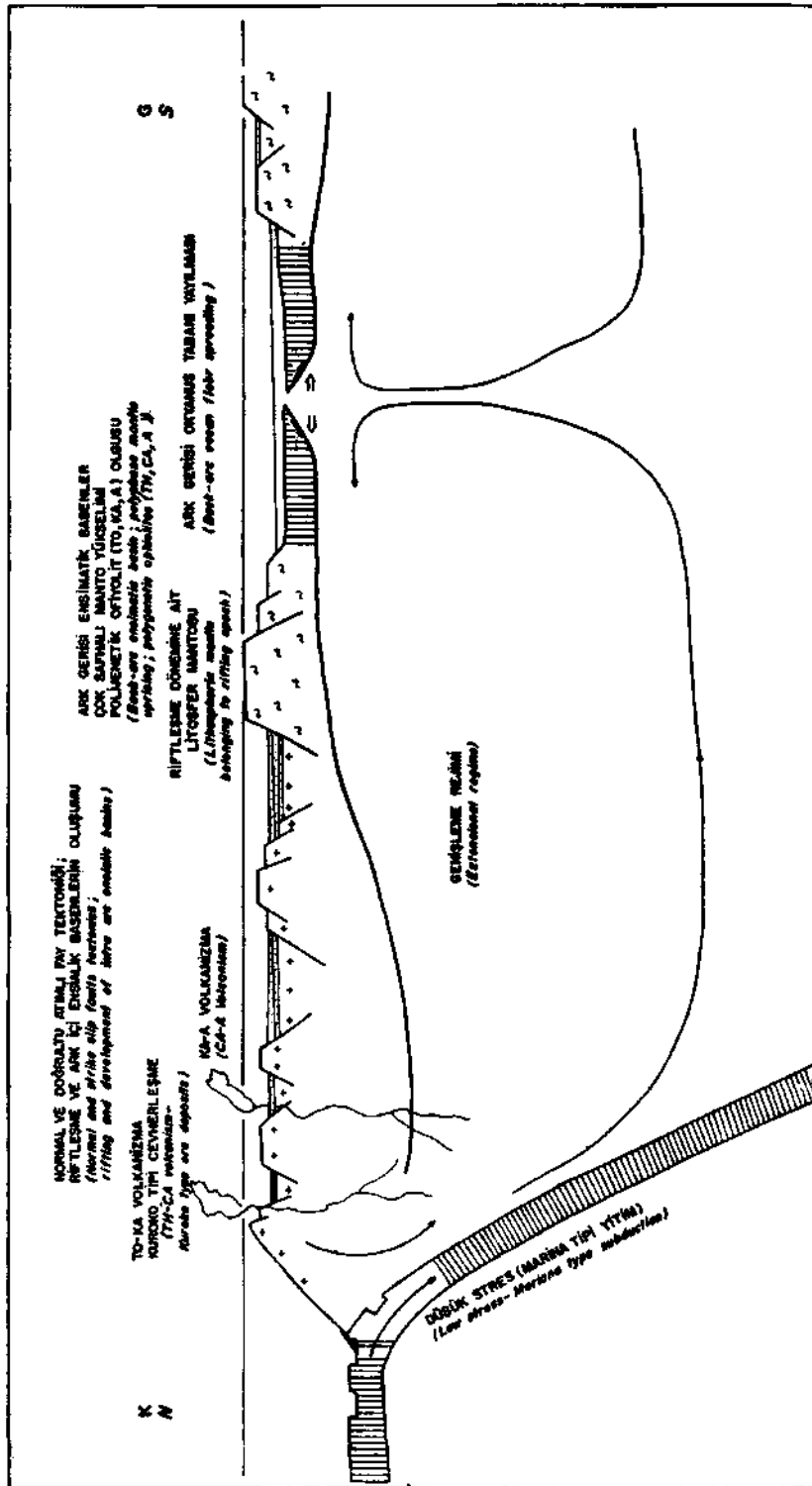According to the geological and geophysical investigations carried out in modern active plate margins, the compressional stresses about 1000 km in the inner part of the overriding plate are the results of interplate friction surfaces in consumption zones (Forsyth, 1975; Isacks and Barazangi, 1977; Uyeda and Kanamori, 1979; Uyeda, 1983; Fukao and Yamaoka, 1983; Miller, 1984). Such compressional stresses have great importance in the evaluation of Cordillerian orogenic belt of the Andeans and Northwest America where the collision is too weak or absent. As a summary, multifold extensional and compressional stress regimes alternated in Eastern Pontides during Mesozoic and Cenozoic. In relation to these regimes, the maximum horizontal compressional stresses (s1) acting in consumption direction (N-S) caused closure of previous basins, folding of basement rocks and sediments and uplift by reverse faults and later the horizontal extensional stresses (s2) caused the opening of new sedimentary basins and new ocean floor spreadings (Fig. 6 and 7). s1 is vertical during this period. These two different tectonic regimes developed Chilean and Marina type con- sumptions (Figure 6 and 7). This implies that a tectonic regime without collision was active in Eastern Pontides during Mesozoic. But the presence of Cimmeridianr orogenic phase (Şengör et al., 1980) due to the collision of Eurasia continent and Pontides in Dogger (closure of Paleotethys) is doubtful in Eastern Pontides. Such a collision should result in backarc compressional stresses and related backarc thrust or reversal of consumption such as it is-in modern Sunda arc (Silver et al., 1983). However, it has been proved by geological evidences that there existed an extensional stress regime during Dogger-Malm and Lower Cretaceous in Eastern Pontides (Şengör et al., 1980; Bektaş et al., 1984). Nevertheless, it is possible that new basins were developed between uprising blocks throughout the Pontides or synchronous compressional and tensional stresses may be active in adjacent areas. Such a tectonic regime is typical for the strike slip fault zones (Aydın and Nur, 1982). This is checked by the presence of some basins during compressional stress and extensional stress periods.

The general analyses of elements of Eastern Pontides (fold, fault and dyke systems) reveal that the compressional stress periods developed in a similar fashion (during Mesozoic and Ceno- zoic) but the maximum compressional stress showed direction variations up to 90°. In fact, it is known that the Upper Cretaceous sediments in the northern part of Eastern Pondites have steep fold axes (Turkish-Japanese team, 1974; Altun, 1977). This work reveals that the same situation is valid for the southern part. It was reported that compressional stresses had formed folds at right angles (N115-145E and N00-40) in the Agean arc during Upper Miocene and Lower Pliocene (Mer- cier, 1981) and the maximum compressional stresses in Middle America have directions of 310±10 and 80 (Kellog and Bonini, 1982). On the other hand, Hida mountains, the highest mountain range of Japan on the coast of Japan Sea, has reached a height of 2000 m (1-5 mm/year) since the late Tertiary. The main cause of this uplift is maximum compressional stresses being in the consumption direction and directional variations from NW-SE to WNW-ESE (Fucao and Yamaoka, 1983). As suggested by Yamakawa and Takahashi (1977) the bisectrix of stresses in various directions, perpen- dicular to the structural belt defined by strike-slip tectonics, corresponds to the direction of maximum stress. The evidence given above shows that the main causes of the variation of compressional stress directions are the variations in plate movements and the strike-slip faulting on the overriding plate. From this point of view, the mechanics of maximum compressional stresses in NW-SE and NE-SW directions is compatible with strike-slip faulting in Eastern Pontides during Mesozoic and Cenozoic. The real tectonic compressional stresses are perpendicular to the Pontid mountain range and are in the direction intersecting these different directions. This is the same with consumption direction in periods mentioned above. In the consumption zone, the development of horizontal compressional

stresses of relatively lower intensity, due to plate movements and the transmission of these stresses to Southern Pontides in E-W direction with a decreasing intensity, have caused oblique and occasional strike slip faulting in this region. This period corresponds to the time when vertical stresses were generally greater than the horizontal ones.

As a summary, during Mesozoic, Eastern Pontides had an uncollisional tectonic regime such as the Andean and the Cordillerian orogenic belts. In such tectonic regimes, the source of maximum compressional stresses is consumption zones. Since the plates are not rigid, such horizontal compressional stresses are transmitted from the front margin to the inner parts of plates with a decreasing intensity. Therefore we observe the maximum compressional stresses in front margins and extensional stresses in backarc regions. During Mesozoic, an extensional stress regime except for very short periods of compressional stresses existed in the Eastern Pontian arc and as a result of this phenomenon especially in Southern Pontides a polyphase rifting and ocean floor spreading developed. The development of such events in Southern Pontides implies the evolution of the Eastern Pontides on a southward subduction. The N-S directed main tectonic compressional stress, the bisectrix of NW-SE and NE-SW maximum compressional stresses, was in the subduction direction and caused strike slip fault zones in arc and backarc regions.

Manuscript received May 20, 1985

REFERENCES

Adamia, SH. A.; Lordkipanidze, M.B. and Zakariadze, G.S., 1977, Evolution of active continental margin as exemplified by the Alpine history of the Caucasus: Tectonophysics, 40, 183-199.

Akyürek, B.; Bilginer, E.; Akbaş, B.; Hepşen, N.; Pehlivan, Ş.; Sunu, O.; Soysal ,Y.; Dağer, Z.; Çatal, E.; Sözeri, B.; Yıldırım, H. and Hakyemez, Y., 1984, The main geological features of Ankara-Elmadağ-Kalecik region: JMO Bull.,20, 31-46 (in Turkish).

Altun, Y., 1977, Geology of Çayeli-Madenköy copper-zinc deposit and problems related to mineralization: MTA Bull., 89, 9-22 (in Turkish), Ankara-Turkey.

Aydın, A. and Nur, A., 1982, Evolution of pull-apart basins and their scale: Tectonics, 1,91-107.

Bektaş, O., 1981, The geological features of North Anatolian Fault Zone in Erzincan-Tanyeri district and local ophiolite problems: Karadeniz University, Faculty of Earth Sciences 32, 196 p. (in Turkish).

————, 1982, The paleotectonic setting of trondjhemites associated to Tanyeri (Erzincan) ophiolite complex and their origins: Karadeniz University, Earth Sciences Bull., 2, 39-51 (in Turkish), Trabzon-Turkey.

————, 1983, (I) type granitic rocks in the eastern Northern Pontid magmatic arc and their geotectonic setting: Geo. Soc. of Turkey, 37 th Scientific and Technical Congress, Abstracts, 49-50 (in Turkish).

————1984, The shoshonitic volcanism of Upper Cretaceous age in Eastern Pontides and its geotectonic importance: Karadeniz University, Earth Sciences Bull., 3, 1-2, 53-62 (in Turkish), Trabzon-Turkey.

————; Pelin, S. and Korkmaz, S., 1984, Mantle uprising in Eastern Pontid back-arc basin and the concept of polygenetic ophiolite: Geo. Soc. of Turkey, 38th Scientific and Technical Congress, İhsan Ketin Symposium (in Turkish).

Cochran, J.R., 1983, A model for development of Red-Sea: Am. Assoc. of Petr. Geol. Bull., 67, 41-69.

Desheng, L, 1984, Geological evolution of petroliferous basins on continental shelf of China: Am. Assoc. of Petr. Geol. Bull., 68, 993-1003.

Dewey, J.F.; Pitman W.C.; Ryan, W.B.F. and Bonnin, J., 1973, Plate tectonics and evolution of Alpine system: Geol. Soc. Am. Bull., 84, 3137-3180.

Eğin, D. and Hirst, D.M., 1979, Tectonic and magmatic evolution of volcanic rocks from the northern Harşit area, NE Turkey: Geocome-I, Min. Res. and Expl. Inst., Geo. Soc. of Turkey, 56-94.

Engelder, T. and Geiser, P., 1980, On the use of regional joint sets as trajectories of paleostress fields during the development of the Appalachian Plateau New York: Jour, of Geophys. Res., 86, 6319-6342.

Eren, M., 1983, Geology of the area between Gümüşhane and Kale and microfacies analysis of the region: Master Thesis, Karadeniz University, Faculty of Earth Sciences, 197 p. (in Turkish), Trabzon-Turkey.

Forsyth, D.W., 1975, Fault plane solutions and tectonics of the South Atlantic and Scotia Sea: Jour. Geophys. Res., 80, 1429-1443.

Frisch, W., 1979, Tectonic progradarion and plate tectonic evolution of Alps: Tectonophysics, 60, 121-139.

Fukao, Y. and Yamaoka, K., 1983, Stress estimate for the highest mountain system in Japan: Tectonics, 2, 453-473.

Gattinger, T., 1962, Explanation text of geological map of Turkey, Trabzon (1:500 000): MTA Publ., Ankara-Turkey.

Gedikoğlu, A.; Pelin, S. and Özsayar, T., 1979, The main lines of geotectonic development of East Pontids in the Mesozoic era: Geocome-I, Min. Res. and Exp. Inst., Geol. Soc. of Turkey, 551-581, Ankara-Turkey.

Görür, N.; Şengör, A.M.C.; Akkök, R. and Yılmaz, Y., 1983, Sedimentological evidence related to the northern part of Neo-Tethys in Pontides: Bull, of Geol. Soc. of Turkey, 26, 11-21 (in Turkish).

Hacıalioğlu, T., 1983, The geology and microfacies analysis of the area between Kale and Vavuk Dağı (Gümüşhane): Master Thesis, Karadeniz University, Faculty of Earth Sciences, 121p. (in Turkish), Trabzon-Turkey.

Isacks, B.L. and Barazangi, M., 1977, Geometry of Benioff zones lateral segmentation and downward bending of the subducted litosphere in Island arc, Deep Sea Trenchs and Back-arc basins: Maurice Ewing Ser., 1, 99-114.

Kellogg, J.N. and Bonini, W.E., 1982, Subduction of the Caribbean plate and basement uplifts in the overriding South American Plate: Tectonics, 1, 251-277.

Ketin, İ., 1:500 000 scaled geological map of Turkey, Sinop: MTA Publ., Ankara-Turkey.

Kronberg, P., 1969, Bruchtektonik im Ostpontischen Gebirge (NO-Turkei): Geol. Runds., 59, 257-265.

Le Blanc, M., 1981, The late Proterozoic ophiolites of Bau Azzer (Morocco): Evidence for Pan-African plate tectonics: In: A. Kroner (ed), Precambrianplate tectonics, Elsevier, Amsterdam, 435-451.

McKenzie, D.P., 1978, Some remarks on the development of the sedimentary basins: Earth Planetary Sci. Letters, 40, 25-32.

Mercier, J.L., 1981, Extensional compressional tectonics associated with the Agean arc: Comparison with the Andean Cordillera of south Peru-North Bolivia: Phil. Trans. R. Soc. Lond. A 300, 337-357.

Miller, H., 1984, Orogenic development of Argentinian Chilean Andes during the Paleozoic: J. Geol. Soc. London, 141, 885-892.

Moores, E.M.; Robinson, P.T.; Malpas, J. and Yenophonotos, C., 1984, Model for the origin of the Troodos massif, Cyprus, and other mideast ophiolites: Geology, 12, 500-503.

Mukhopadhyay, M., 1984, Seismotectonics of subduction and back-arc rifting under the Andaman Sea: Tectonophysics, 108, 229-239.

Nakamura, K. and Uyeda, S., 1980, Stress gradient in arc/back-arc regions and plate subduction: Jour, of Geophys. Res., 85, 6419-6428.

Nebert, K., 1961, Geology of the region comprising Kelkit and Kızılırmak valleys (N Anatolia): MTA Bull., 57, 1-49 (in Turkish), Ankara-Turkey.

Öztürk, A., 1980, Tectonics of Ladik-Destek region: Bull, of Geol. Soc. of Turkey, 2-3, 1, 31-39 (in Turkish).

Pelin, S., 1977, The geological investigation for petroleum possibilities in the southeastern Alucra (Giresun): Karadeniz University, Faculty of Earth Sciences, 13 (in Turkish), Trabzon-Turkey.

Saner, S., 1930, The explanation of the formation of Eastern Pontides and adjacent basins by using plate tectonics concept, NW Turkey: MTA Bull., 93/94, 1-20 (in Turkish), Ankara-Turkey.

Schultze-Westrum, H.H., 1961, The geological profile of Aksu stream near Giresun: MTA Publ., 57, 63-71 (in Turkish), Ankara-Turkey.

Seymen İ., 1975, The tectonic characteristic of North Anatolian Fault Zone in Kelkit valley region: Istanbul Tech. Univ., Mining Department, 192 p (in Turkish), Istanbul-Turkey.

Silver, E.A.; Reed, D.; McCaffrey, R. and Joyodiwiryo, Y., 1983, Back-arc thrusting in the Eastern Sunda arc, Indonesia: A Consequence of arc-continent collision: Jour, of Geophys. Res., 88, 7429-7448.

Şengör, A.M.C.; Yılmaz, Y. and Ketin, İ., 1980, Remnants of a pre-Late Jurassic ocean in Northern Turkey: Fragments of a Permian Triassic Paleo-Tethys: Geol. Soc. Am. Bull., 91, 599-609.

Terlemez, I. and Yılmaz, A., 1979, The stratigraphy of the area between Ünye, Ordu, Koyulhisar and Reşadiye: Bull, of Geol. Soc. of Turkey, 23/2, 179-193 (in Turkish).

Terzioğlu, M.N., 1984, The petrology and geochemistry of Bayırköy volcanics of Eocene age in the south of Ordu: Karadeniz University, Eng. and Arch. Faculty, Bulletin of Earth Sciences, 1, 44-57 (in Turkish),Trabzon-Turkey.

Tokel, S., 1981, Magmatic emplacements and geochemistry in Plate Tectonics: Examples from Turkey: Yeryuvarı ve İnsan, 6/3-4, 53-65 (in Turkish).

Trumpy, R., 1981, Alpine paleography-a reappraisal: Paper presented at the Mountain building symposium, Zurich, July, 1981, 14-18.

Turan, M., 1978, The geology of east of Şiran (Gümüşhane): Master Thesis, Karadeniz University, Faculty of Earth Sciences, 57 p (in Turkish), Trabzon-Turkey.

Turcotte, D.Z., 1983, Mechanism of crustal deformation: The Geological Society, Thirty-Sixth William Smith Lecture, 701-717.

Turkish-Japanese Team, 1974, Report on geological survey of Trabzon Area, Northeastern Turkey Phase I: MTA Rep., (unpublished), Ankara-Turkey.

Uyeda, S., 1983, Comparative subductology: Episodes, 2, 19-24.

————and Kanamori, H., 1979, Back-arc opening and the mode of subduction; Jour, of Geophys. Res., 84, 1049-1061.

Ünalan, G. and Yüksel, V., 1978, An example of ancient grabens: Haymana-Polatlı basin: Bull, of Geol. Soc. of Turkey, 21, 159-165 (in Turkish).

Vink, G.E.; Morgan, W.J. and Zhao, W.L., 1984, Preferential rifting of continents: A source of displaced Terranes-Jour, of Geophys. Res., 89, 10072-10077.

Wilson, J.T., 1968, Static or mobile earth: The current scientific revolution: Am. Philos. Soc. Proc., 112, 309-320.

Yamakawa, N. and Takashashi, M., 1977 Stress field in focal regions with reference to the Matsumoto earthquake swarm: Pap. Meteorol. Geophys., 28, 125-138,

Yıldız, B., 1984, The relation of various structures to the Cu, Pb, Zn mineralization in Eastern Black Sea Region recognized by photogeplogical means: MTA Bull., 89/100, 92-98 (in Turkish), Ankara-Turkey.

Winterer, E.L. and Bosellini, A., 1981, Subsidence and sedimentation on Jurassic passive continental margin Southern Alps, Italy: Am. Assoc. Petr. Geol. Bull., 65, 394-421.

Zoback, M.L. and Zoback, M., 1980, State of stress in Conterminous United States: Jour, of Geophys. Res., 86, 6113-6157.

Zwart, H.J. and Dornsiepen, V.F., 1978, The tectonic framework of Central and Western Europe: Geol. Mijnbouw, 57, 627-654.

THE GEOLOGY OF AROUND ESKİŞEHİR AND THERMAL WATER SOURCES

M. Ziya GÖZLER**; Fahrettin CEVHER*** and Arif KÜÇÜKAYMAN***

ABSTRACT.— The investigated area comprises Eskişehir province and its immediate vicinitiy. The basement consist of Pre-Triassic tectonic unit comprising metamorphic, ophiolitic and metadetritics. Jurassic is represented by detritics and limestones. These are unconformably overlain by sediments and volcanic rocks of Paleocene, Eocene, Miocene and Pliocene age. The uppermost unit consist of sandstones of Pleistocene age. The magmatic rocks are respectively represented by porpyritic granite and an assemblage of andesite, bazalt and tüff. The vertical fault systems passing throuh north of Eskişehir, responsible for the present morphology trends E-W and the northern and southern system dip respectively to the S and N the reverse faulting of the region is belived to have played and important role in the tectonic evolution of studiee area.

HYDROTHERMAL ALTERATION STUDY AND VOLCANIC ROCK PETROLOGY OF ÇANAKKALE-TUZLA GEOTHERMAL AREA

A. İhsan GEVREK*; Mehmet ŞENER* and Tuncay ERCAN***

ABSTRACT.— Hydrothermal alteration zones have been investigated by x-ray diffraction techniques and geochemical analysis. In studied area; alunite, kaolinite, montmorillonite, illite, and silica zones have been recognized. These hydrothermal alteration zones indicate that there are geothermal fluids which have a temperature of 150-225Co in the reservoir. The tectonic structure of studied area is developed by NW-SE and NE-SW directional forces. Geothermal fluids coming from the diagonal cracks formed as a result of faults having a strike of E-W and formed as a result of these forces have formed the necessary environment for hydrothermal alteration. Volcanic rocks where hydrothermal zones are observed in the studied area are of Lower-Middle Miocene age and are represented by latite, andesite, dacite, rhyolite type lavas and tuff and ignimbrites. With petrochemical studies it has been concluded that volcanites are an inner continental volcanism having calc-alkaline with high potssium and schoshonitic proporties and are shelf characteristic.

THE GENESIS OF ESKİŞEHİR-BEYLİKAHIR COMPLEX FLUORITE DEPOSIT AND PRELIMINARY BENEFICIATION STUDIES

M. Sabri ÇİFTÇİ*

ABSTRACT.— This paper describes beneficiation studies of a complex fluorite ore containing considerable amount of barite as well as rare earth minerals. The deposit is located at Eskişehir-Beylikahır district, West of Turkey. Genesis of the ore is thought to be hydrothermal. Following the characterization studies, the liberation size of relatively coarse fluorite was found to be minus 0.15 mm at which approximately 40 % of the total fluorite was liberated. Obtaining a higher degree of liberation does not seem to be possible owing to the micro and cripto crystalline form of the rest of fluorite. As accessory minerals, calcite, quartz, ironhydroxides, psilomelane, muscovite and some clay minerals have also been determined. The liberated fluorite was concentrated by gravity (shaking table) and flotation methods. Acceptable concentrates have been obtained for metallurgical, glass and ceramics industries.

LIQUEFACTION CHARACTERISTICS OF TURKISH LIGNITES

Kılıçaslan N. BAYRAKTAR and Olcay ÖZKAPLAN*

ABSTRACT.— Samples of Beypazarı, Elbistan and Kangal were hydrogenated in a bomb reactor, in the presence of tetralin and without catalyst, under 395°C temperature and 7MPa cold hydrogen pressure conditions for 17 minutes. Conversion, liquid yield and preasphaltenes-asphaltenes-oil distribution were determined by a standardized procedure. The Beypazarı sample gave higher conversion (91 %) and liquid yield (64 %) in comparison with the others, but the lightest liquid was derived from Elbistan sample. The consistency of the experiment was verified by total mass and sulphur balances, which gave closures around 100 %.

INTRODUCTION

The estimated maximum life of 50 years of world oil reserves (Bayraktar and Özkaplan, 1982) and the reality that oil can be used as a political weapon have rendered coal liquefaction, i.e. the use of coal for the production of petroleum-like liquids, an important issue. Today the only plant which liquefies coal commercially is SASOL in South Africa, where coal reserves are rich and manpower is cheap. Various liquefaction processes are presently under development in the USA, Great Britain, Federal Germany, USSR, and Japan. The commercialization of many of these processes is now dependent almost only on the price of oil.

This report describes the first step of a project undertaken to investigate the liquefaction behaviour of Turkish lignites with reserves greater than 100×10^6 tonnes. At this stage, the amenability to hydroliquefaction under standardized conditions is examined and compared. With regard to reaction approach, the treatment resembles EDS, SRC and CSF processes (Bayraktar and Özkaplan, 1982). Initially, samples from three sites, viz. Ankara-Beypazarı, Maraş-Elbistan and Sivas-Kangal, which have strategic importance because of their geographical locations, were investigated.

EXPERIMENTAL SECTION

1. Preparation of the samples

The samples were freshly taken from the coal face and various representative size fractions were prepared keeping exposure to a minimum (Fig. 1). Optimization between time, labour and particle size homogeneity was done at every stage of the size reduction programme. The —0.2 mm (—200 mm) samples used in the experiments were stored in plastic containers and purged with nitrogen twice a month against oxidation.

2. Characterization of the samples

Unless otherwise stated, it should be understood that all determinations have been made in duplicate and the average reported.
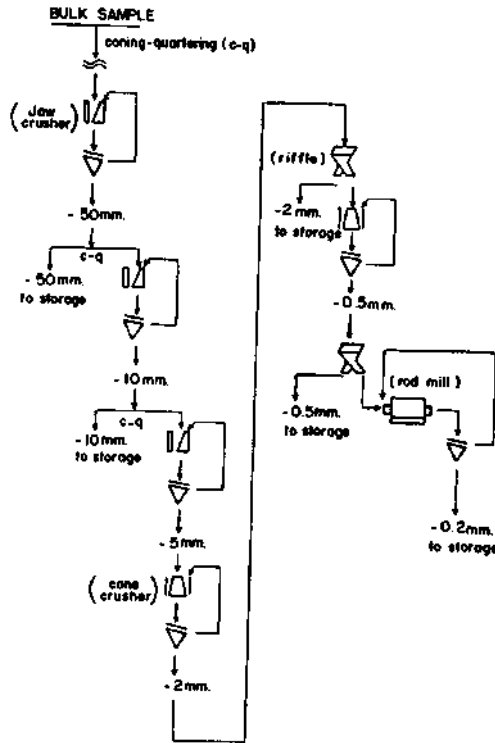
Fig. 1 - Size reduction flowsheet.

a. Particle size analyses were carried out as per ASTM D197. The results are in Table 1. Repeatability of the fraction percentages were better than ±0.5.

b. Chemical, calorific and petrographic data are given in Tables 2,3,4,5.

Moisture was calculated from the weight loss that 1 g of sample underwent at 105-110°C under 0.10 kPa in two hours. Repeatability was better than ± 1 % of the reported value.

Standard ash content was determined as per TS 1042. In order to minimize mineral decompusition and obtain an ash value representing mineral matter more, closely, ash was additionally determined at 520°C. The tolerance of the 520°C-ash was ± 1 %.

Table 1 – Particle size analyses

Lignite	Beypazarı	Elbistan	Kangal
Moisture (%)	14.0	16.1	12.4
+ 212 μm	4.2	3.6	8.4
— 212 + 150 μm	20.3	20.6	8.6
— 150 + 106 μm	14.2	14.9	18.2
— 106 + 75 μm	18.7	12.5	13.9
— 75 + 63 μm	8.4	5.9	6.8
— 63 μm	34.2	42.5	44.1

Table 2 - Standard characteristics of the samples

% Moisture-free basis	Beypazarı	Elbistan	Kangal
Ash	39.4	32.1	44.4
VM*	31.0	44.0	27.3
Fixed carbon (diff.)	29.6	23.9	28.3
Ash (520°C)	40.4	39.9	45.2
Mineral CO_2	0.66	7.8	0.30
C	42.0	42.0	36.0
H	3.17	2.77	2.93
N	1.17	1.12	0.93
S (total)	4.72	3.16	0.67
O (diff.)**	11.4	11.7	15.2
Sulphate S	0.97	0.21	0.08
Pyritic S	1.53	0.45	0.34
Organic S (diff.)	2.22	2.50	0.25
Gross calorific value (MJ/kg)	16.72	16.15	13.96
H/C (atomic)	0.907	0.791	0.977
"O"/C (atomic)	0.20	0.21	0.32

* Uncorrected for mineral CO_2.
** $100 - C - H - N - S_{org} - ash - mineral\ CO_2$.

Table 3 - Petrographic properties of the samples

Meceral group (volume %, organic basis)	Beypazarı	Elbistan	Kangal
Huminite (vitrinite)	89.0	89.2	72.2
Liptinite (exinite)	10.2	10.0	17.7
Inertinite	0.8	0.8	10.1
% $\overline{R}m$*	0.38	0.30	0.20

* Mean maximum vitrinite reflactance.

Table 4 - Ash analyses of the samples

% in 815°C-ash	Beypazarı	Elbistan	Kangal
SiO_2	48.7	15.6	71.1
Al_2O_3	18.1	7.7	7.5
Fe_2O_3	11.6	4.5	4.8
CaO	4.3	46.6	10.6
MgO	2.7	3.1	2.0
Na_2O	6.3	0.26	0.59
K_2O	1.3	0.38	0.67
TiO_2	0.87	0.87	0.65
SO_3	5.1	19.7	2.5

Table 5 - Rational analyses of the samples

%, Organic basis	Beypazarı	Elbistan	Kangal
Bitumen	4.0	5.7	4.3
Humic acids	14.0	57.2	21.1
Lignin-type constituents	82.0	35.1	74.6
Cellulosics	0.0	2.0	0.0

Volatile matter (VM) was found under the conditions given in TS 711, however on a pelletized sample in order to prevent «sparking» (Montgomery, 1978).

Mineral CO_2, necessary for correction of VM and carbon, was measured by ASTM D 1756 and TS 1044 (11).

Carbon and hydrogen determinations were carried out on a semi-micro scale by a high-temperature method in the Laboratories Dept. of MTA. Carbon was corrected for CO_2 from minerals. Nitrogen and total sulphur were determined as per TS 362 and TS 363 respectively.

In the determination of sulphur forms, BS 1016/11 was followed owing to its simplicity.

Gross calorific value was measured as per ASTM D 2015

Ash analysis was performed on 815°C - ash by wet chemical techniques in the Laboratories Dept. of MTA.

Petrographic and rational analysis was conducted in the Faculty of Chemistry of Hacettepe University (TÜBİTAK project, 1984).

3. Experimental set-up and procedure

Samples of particle size —200 mm were hydrogenated in a reaction bomb, in the presence of tetralin and without catalyst, under 395°C temperature and 6.9 MPa initial hydrogen pressure conditions for 17 minutes. Under these mild conditions the liquefaction performances of the lignites were distinguishable.

a. Apparatus: The liquefaction system is schematically illustrated in Figure 2. The hydrogenations were carried out in two identical PARR 4740 bombs (316 S.S.) of 71 mL capacity. A TECHNE SBL-2 fluidized sand bath with provisions for temperature control was used as the heat source. The bomb was shaken in the sand bath along its longitudinal axis at 4 cm amplitude and 400 cycles per minute frequency. Upon termination of the experiment, the bomb was immersed into the adjacent cold water bath to accomplish rapid cooling.

Since the construction of the bomb prohibited the use of an internal thermocouple, the inside temperature was calibrated against the bomb surface temperature. In calibration experiments the charge was simulated with tetralin/coke mixtures. Eventually the temperatures and durations of heat-up, reaction, and cool-down were estimated with good reproducibility.

b. Procedure: The procedure was developed to obtain as many data as possible in a short time. Typically, a test is completed in ten hours.

All chemicals were used as supplied. Unless otherwise stated, the sensitivity of the weighings was 0.01 g.

15 g (W_T) of tetralin and a quantity of—200 mm air-dried lignite sample, corresponding to 7.5 g (W_C) on a moisture-free (mf) basis, are transferred into the bomb. The bomb is assembled, purged twice with hydrogen, and pressurized to 6.9 MPa with hydrogen. After a pressure test of at least two hours, it is immersed into the sand bath preheated to about 450°C and shaking is initiated. The temperature of the sand bath is continuously monitored, by addition of cold sand or adjustment of the temperature controller, according to the temperature calibrations. On completion of the appointed reaction time, the bomb is quickly quenched to room temperature by immersion into the cold water bath. Typical heat-up reaction, and cool-down times are 10, 17, and 10 minutes respectively.
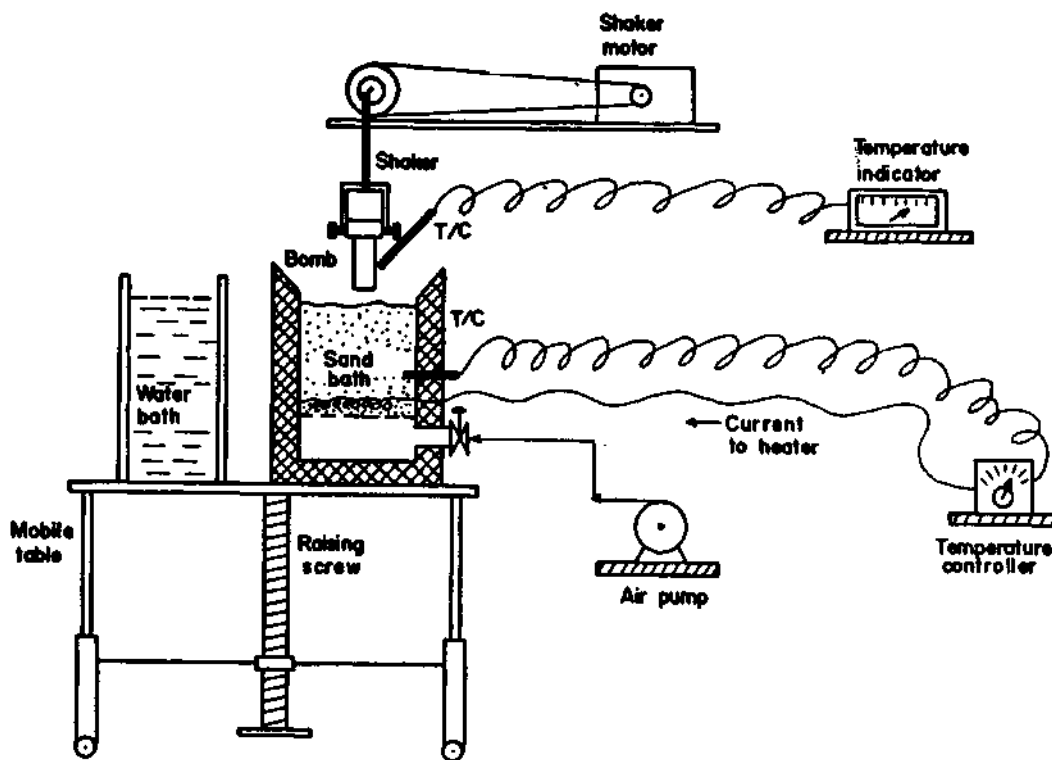
Fig. 2 - Liquefaction system.

Final bomb pressure is measured. If total mass and sulphur balances are to be made, the gas is passed through an absorption train for characterization (see Addendum); otherwise it is discarded.

The bomb contents are washed quantitatively into a beaker with fresh THF (tetrahydrofuran). The mixture is preserved under nitrogen in the refrigerator overnight.

The succeeding operations are shown in the form of a flowchart in Figure 3. The slurry is filtered through Whatman no: 42 or 44 paper (pore size: 2.5 mm) in a Buchner funnel. The residue is dried at 105-110°C and 0.10 kPa for 2 h and weighed (W_R) for calculation of total conversion (C_t). Soxhlet extraction has been found superfluous after a number of comparative experiments.

The filtrate is concentrated following a temperature programme (maximum: 80°C) in a HEINO S rotary evaporator under nitrogen sweep. It has been experimentally verified that water in the filtrate is removed practically completely as water-THF azeotrope under these conditions. Evaporation is continued until a concentrate of ca. 50 % THF is obtained, and this concentrate is weighed (W_{CON}).

The THF content of the concentrate is estimated chromatographically. The operating characteristics are as follows:

```
Chromatograph          :PACKARD-BECKER          Model 419
Column                 :2           m X 1/4", 15 % Apiezon-L on 80-100 Chrom W
Detector               :TC,         240°C, 250 mA
Carrier gas            :He,         20 mL/min (at 20°C)
Injection temperature          :240°C
Sample quantity        :5.00±0.05          mL
Attenuation                    :64
Temperature programme  :100°C  -    240°C, stepwise
```

Fig. 3 - Product work-up.
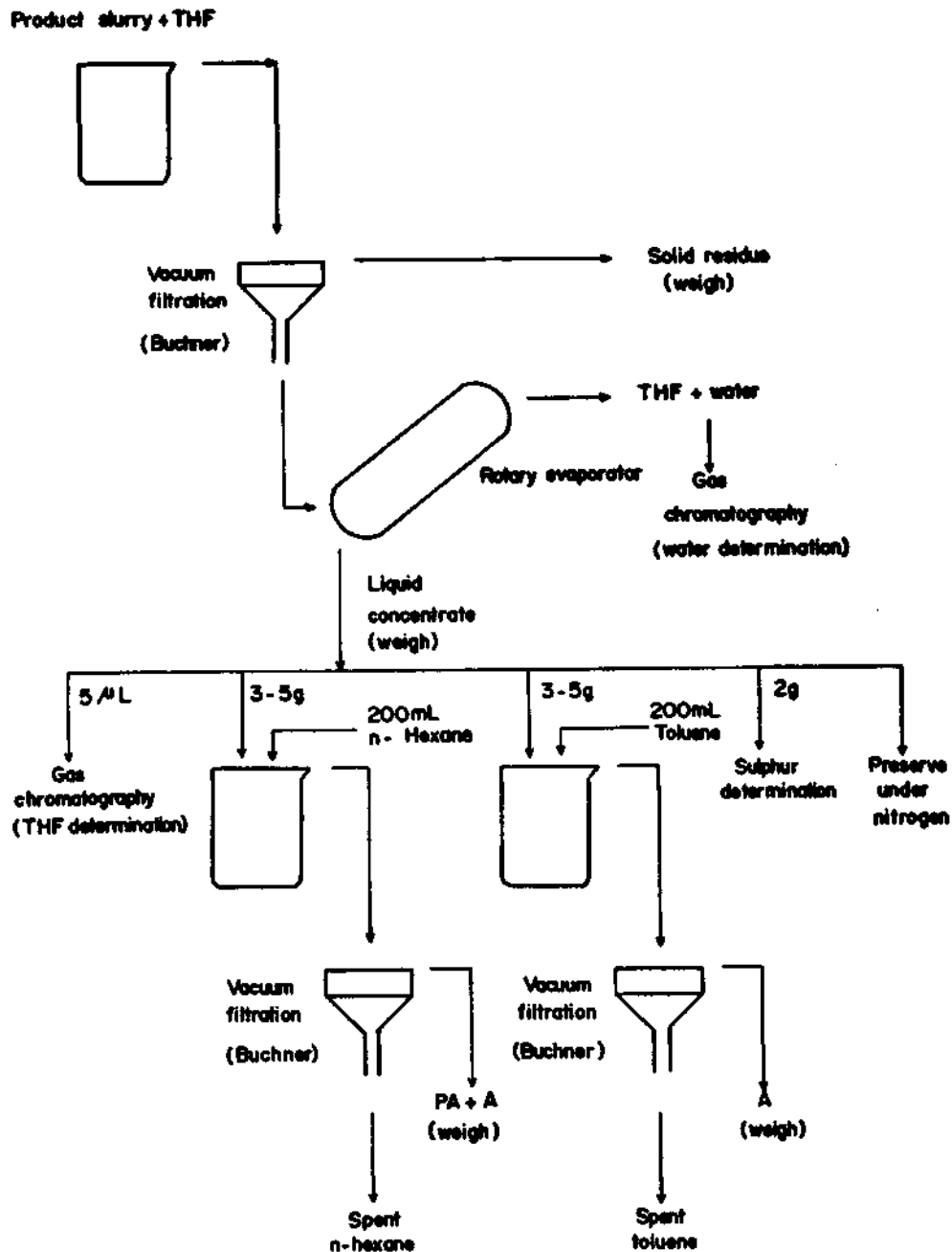
As a result of such operation, THF and tetralin yield tall and sharp peaks, and probable near-boiling materials such as hexane, benzene, toluene and decalin, naphthalene are nicely separated.

The THF content of the concentrate (X_{THF}) is determined by matching with similar standard mixtures, and the quantity of coal liquid (W_L) and liquid yield (L) are calculated therefrom.

Two aliquots of 3-5 g (T and H) are pipetted from the concentrate, and 200 mL of toluene and 200 mL of n-hexane are added respectively. After 30 minutes of standing, the two mixtures are filtered as in the case of bomb washings and the precipitates washed copiously with the respective solvents. The «preasphaltene» precipitate (t) from toluene precipitation and the preasphaltene+asphaltene' precipitate (h) from n-hexane precipitation are dried at 105-110°C and 0.10 kPa for one hour and weighed to a sensitivity of 0.1 mg. The preasphaltene-asphaltene-oil distribution is then computed.

Sulphur content of the coal liquid is determined on a 1 g sample of concentrate in a Leco Analyzer in the Laboratories Dept. of MTA.

c. Calculation of results

Conversion: Cold THF solubles+gases

$$C_t = \frac{W_C - W_R}{W_C} \times 100 (1-a)$$

W_C : Quantity of lignite sample charged (mf)

W_R : Quantity of solid residue (mf)

a   : Fractional ash content of lignite (mf)

C_t : Conversion (% , maf)

Involved error is $\pm$ 0.5 % of the value.

Liquid yield: Product which is soluble in cold THF and boils above 80°C

$$W_L = W_{CON} (1-X_{THF})-W_T$$

$$L = \frac{WL}{W_C(1-a)} \times 100$$

W_{CON} :   Quantity of concentrate

X_{THF} :Fractional   THF content of concentrate

W_T :Tetralin   charged

W_L :Quantity   of coal liquid obtained

W_C :Quantity   of lignite sample charged (mf)

a   :Fractional   ash content of lignite (mf)

L   :Liquid   yield (%, maf)

Here it is assumed that tetralin gives no gaseous product, i.e. that itself and all its reaction products remain in-liquid. It has indeed been reported that deromposition of tetralin to gases is insignificant under these conditions (Charlesworth, 1980). Besides it is a precondition for a viable process that generates as much solvent as it consumes.

Error in liquid yield arises mainly from the quantity of chromatography sample, which bears the largest theoretical error. The error is ± 7 % of the liquid yield for an injection of 5 ± 0.05 mL.

Distribution of preasphaltene-asphaltene-oil: Preasphaltene, liquid component soluble in THF and insoluble in toluene; asphaltene, liquid component soluble in THF and toluene and insoluble in n-hexane; oil, liquid component soluble in all three

$$PA = \left(\frac{t}{T}\right)\left(\frac{W_{CON}}{W_L}\right) \times 100$$

$$A = \left(\frac{h}{H}\right)\left(\frac{W_{CON}}{W_L}\right) \times 100 - PA$$

$$\emptyset = 100 - PA - A$$

t   : Quantity   of precipitate from toluene precipitation

T   : Quantity   of sample for toluene precipitation

W_{CON} : Quantity of concentrate

W_L : Quantity   of coal liquid obtained

h   : Quantity   of precipitate from n-hexane precipitation.

H   : Quantity   of sample for n - hexane precipitation

PA, A,f : Preasphaltene, asphaltene, oil (% of liquid)

The theoretical errors are ± 7,16 and 27 % of the respective values of PA, A and f. These values are affected by the high theoretical error involved in liquid yield.

RESULTS AND DISCUSSION

1. Characteristics of the samples

Particle size analyses (ASTMD 197) of the samples (nominal —200 mm) used in the experiments are given in Table 1.

Although size reduction parameters were optimized, comminution to fines inevitably occurred to some extent. However, it is established that particle size at these levels does not influence the liquefaction reaction (Curran et al., 1967; Pastor et al., 1970; Ruether, 1977; Neavel, 1976; Whitehurst et al., 1980). Tables 2,3,4, and 5 contain the results of the standard characterizations. All the three samples are of high ash, but the ash compositions differ.

The high sulphur contents of Beypazarı and Elbistan samples are prominent. Half of Beypazarı sulphur and three-quarters of Elbistan sulphur are organic in nature, therefore high-sulphur liquids would be expected from these coals.

The atamic H/C ratios are typical for lignites. The ratio is the highest in Kangal lignite, showing agreement with the high exinite content of this sample. Since all the three samples are rich in reactive macerals (vitrinite + exinite), amenability of liquefaction can be expected.

The ash and sulphur contents of the samples are similar to the respective reserve averages (MTA, 1983), but for the extraordinarily low sulphur content of the Kangal sample.

2. Liquefaction findings

The experimental conditions and the main results presented in Table 6. Table 7 contains the results of statistical evaluation.

Table 6 - Liquefaction conditions and results

Sample	Experiment code	Charge lignite (g) /moisture (%) tetralin (g)	Conditions T_r (°C) P_i, P_s (MPa)	Conversion (% maf, 520)	Liquid yield (% maf 520)	PA, A, Ø (% of liquid)
Beypazarı	TARD 6	8.51/11.9 15.00	397 6.91, 5.53	90.3	57.1	47, 33, 20
	TARD 7	8.46/11.3 15.06	391 6.75, 5.59	89.4	64.2	43, 32, 25
	TARD 11	8.42/10.9 15.00	396 6.93, 5.78	92.5	69.6	42, 30, 25
	TARD 16	8.42/10.5 15.01	393 7.01, 5.83	90.0	63.4	43, 37, 20
Elbistan	TARD 9	8.92/15.6 15.05	392 6.78, 6.59	86.8	57.0	19, 29, 52
	TARD 10	8.92/15.6 14.98	396 6.91, 6.73	78.9	51.7	21, 24, 55
	TARD 15	8.59/12.7 15.00	391 7.15, 6.62	78.9	52.3	19, 31, 50
Kangal	TARD 1	8.46/11.8 15.01	398 7.08, 7.02	82.0	43.1	41, 46, 13
	TARD 3	8.46/13.9 15.01	398 7.18, ?	78.4	40.4	49, 39, 12
	TARD 12	8.71/11.9 15.01	399 6.82, ?	83.8	52.6	36, 27, 37
	TARD 13	8.51/11.9 15.00	393 6.85, 6.67	86.7	58.4	32, 28, 40
	TARD 14	8.51/11.6 15.00	392 6.96, 6.84	85.4	46.4	40, 35, 25

T_r - Reaction temperature; P_i - Initial hydrogen pressure (normalized to 20°C);

P_s - Post-reaction pressure (normalized to 20°C); PA- Preasphaltene;

A- Asphaltene; Ø- Oil — reaction time: 17 min.

In the experiments tetralin-to-coal ratio was kept constant at 2:1 on a moisture-free basis. Since the effect of moisture level on charge volume was found negligible, hydrogen to charge ratio should remain nearly constant. Although the difference in moisture levels would give rise to slight differences in hydrogen partial pressures during reaction, this would probably not affect conversion and liquefaction characteristics at this pressure level and in the presence of sufficient hydrogen-donor (Morita et al., 1979; Kamiya et al., 1978).

In expressing the experimental results on a moisture- and ash-free basis, the 520°C-ash values are used. At this ashing temperature carbonates would remain intact but the majority of ashing reactions would reach completion. As can be seen in Table 8, use of the standard high-temperature ash gives rise to artificially low results, particularly for samples such as Elbistan which contain hgh proportions of unstable minerals.

Table 7 - Evaluation of liquefaction results (means and standard deviations)

	Beypazarı	Elbistan	Kangal
Tetralin : coal (mf)	2.00 ± 0.01	2.00 ± 0.01	2.00 ± 0.04
Tetralin : coal (maf, 520)	3.36 ± 0.01	3.32 ± 0.01	3.66 ± 0.07
T_r (°C)	394 ± 3	393 ± 3	395 ± 4
P_i (MPa)	6.90 ± 0.11	6.95 ± 0.19	6.96 ± 0.12*
P_s (MPa)	5.68 ± 0.15	6.65 ± 0.07	6.84 ± 0.18*
ΔP (MPa) **	1.22 ± 0.11	0.30 ± 0.20	0.12 ± 0.06*
Conversion (%, maf, 520)	90.6 ± 1.4	81.5 ± 4.6	83.3 ± 3.2
Liquid yield (%, maf, 520)	63.6 ± 5.1	53.7 ± 2.9	48.2 ± 7.3
Gas (diff. %, maf, 520)	27.0 ± 4.4	27.8 ± 1.7	35.1 ± 5.0
PA (% of liquid)	44 ± 2	19 ± 1	40 ± 6
A (% of liquid)	33 ± 3	28 ± 4	35 ± 8
O (diff., % of liquid)	23 ± 4	52 ± 3	25 ± 13
Tetralin recovery (%)	95 ± 1	94 ± 2	93 ± 2

* Only three experiments have been considered; the post-reaction pressures of the other two were not determined.
** $\Delta P = P_i - P_s$

Table 8 - Effect of ash determination temperature on liquefaction data

	Ash determination temperature (°C)	Beypazarı	Elbistan	Kangal
Conversion (%, maf)	520	90.6	81.5	83.3
	815	89.0	72.2	82.1
Liquid yield (%, maf)	520	63.6	53.7	48.2
	815	62.5	47.5	47.5

Table 9 - Total mass and sulphur balances

	Beypazarı (TARD 16)		Elbistan (TARD 15)	
	Mass (g)	Sulphur (g)	Mass (g)	Sulphur (g)
Input				
Coal (mf)	7.54	0.356	7.50	0.256
Water (as moisture)	0.88	—	1.09	—
Tetralin	15.01	—	15.00	—
Hydrogen	0.30	—	0.30	—
Total	23.73	0.356	23.89	0.256
Output				
Solid residue (mf)	3.48	0.193	3.94	0.071
Water	1.47	—	1.29	—
Coal liquid, Tetralin Tetralin derivatives (liq.)	17.86	0.120*	17.36	0.145
CO_2	0.36	—	0.61	—
H_2S	0.045	0.043	0.054	0.051
Other gases	0.39	—	0.56	—
Total	23.61	0.356*	23.81	0.267
Closure (%)	99.5	100*	99.7	104

* Calculated assuming 100 % closure.

The weight loss involved in the conversion of pyrite to pyrrhotite would have an elevating affect on the measured total conversion. Assuming full transformation, the «increase» in total conversion percentages of Beypazarı, Elbistan and Kangal would be 1.3, 0.4, and 0.3 respectively. These maximum expectable values do not exceed the experimental tolerances (Table 7).

In this stage of the research programme, only general comparisons are made. More detailed correlation of lignite properties with liquefaction behaviour is reserved until screening tests on samples from other important sites are completed.

The greatest consistency (i.e. the lowest standard deviations) is associated with Beypazarı with respect to conversion and with Elbistan with respect to liquid yield. All the samples, Beypazarı in particular, give high conversions under these relatively mild reaction conditions. The highest liquid yield is also obtained from Beypazarı sample. The high pyrites content of this lignite may be partly responsible for this superior performance. Liquid selectivity, which can be represented by the percentage ratio of liquid yield to conversion and is, desired to be high, is 70 for Beypazarı, 66 for Elbistan, and 58 for Kangal. Both liquid selectivity and liquid yield follow the same order with mean reflectance values and the reverse order with «oxygen» content. Thus, liquid yield increases with degree of coalification for these three lignites. Gas (+ water), expressed as the difference between conversion and liquid yield, shows the reverse trend. The greater the oxygen content, the more gas the coal would give during liquefaction (Whitehurst et al., 1980; Cudmore, 1977/78).

Beypazarı and Kangal liquids are similar on the basis of preasphaltene -asphaltene-oil distribution. Elbistan liquid, on the other hand, is completely different; it is remarkably «light» with its oil content of 52 %. Preasphaltenes and asphaltenes are composed of undistillable products, contain large proportions of heteroatoms (O,N,S) pose difficulties in catalytic processing,and negatively influence the storage properties of liquids. In short, they are undesirable. It appears that a quarter of Beypazarı and Kangal liquids and one half of Elbistan liquid are potentially distillable. The tendency of Elbistan lignite to yield light liquids was also observed by Bayraktar in an earlier study (Bayraktar, 1981). This would perhaps imply that the molecular structure of Elbistan lignite is made up of small building blocks. Unless the high oil yield is realized at the expense of high hydrogen consumption, Elbistan lignite can be specified as quite amenable to liquefaction. However, the sulphur content of Elbistan liquid is high.

Tetralin recoveries were estimated with reasonable accuracy by gas chromatography. The results indicate that consumption of hydrogen-donor solvent remains low.

Total mass and sulphur balances are given in Table 9. The additional operations required are explained in Addendum.

Attainment of full closure in total mass balances despite the small scale of experimentation signifies the reliability of the present techniques and results. The elements missing from the balance sheet are water left in solid residue and ammonia. It has been found that only very little water can be retained in the residue since water is removed almost quantitavively by THF. Even if all coal nitrogen were converted to ammonia, 0.11 g of ammonia would result; in fact only one-third undergoes such transformation (Bayraktar,1981). Hence significant erros would not ensue when ammonia is neglected; it is very difficult to determine in such minute quantities.

The sulphur balance around one Elbistan experiment also gave good closure. Here the greatest error would be associated with the sulphur of the liquid since it compounds errors from i) determination of coal liquid, ii) sampling a volatitle liquid, and iii) multiplication of the specified precision of the Leco determination (± 2 %) with a large factor. Nevertheless practically full closure of the sulphur balance shows that sulphur content of coal liquid can be calculated reliably from a forced sulphur balance. So was the sulphur in the Beypazarı concentrate calculated in Table 9.

The sulphur contents of the Beypazarı and Elbistan liquids can be calculated as 4.2 and 6:1 % respectively. Such high-sulphur liquids are unlikely to be used without radical desulphurization. The distribution of sulphur into the products are shown in Table 10. In the case of Beypazarı, more than half of the sulphur remains in the residue as expected from lignite of high sulphate and pyritic sulphur. Whereas in Elbistan, whose sulphur is over three-quarters organic more than half of the sulphur reports to the liquid. A similar distribution was found for Elbistan lignite in a previous study (Bayraktar, 1981). A direct linear relationship was observed between organic sulphur in feed coal and sulphur in product liquid (Whitehurst et al., 1980). Pilot-scale experience indicates that sulphur in liquid varies exponentially with hydrogen consumption (Gorin, 1981). In this work, 72 and 68 % respectively of organic sulphur in Beypazarı and Elbistan appear in coal liquid.

Table 10 - Distribution of sulphur into products

Product	% of lignite S	
	Beypazarı (forced balance)	Elbistan
Solid residue	54	27
Coal liquid	34	54
Gas	12	19

Yields of carbon dioxide are 8 and 14 % for. Beypazarı and Elbistan respectively. Thus 30 and 50 % of lignite "oxygen" are removed in the form of carbon dioxide.

CONCLUSION

Lignite samples from three inland deposits (Ankara-Beypazarı, Maraş-Elbistan, Sivas-Kangal) were hydrogenated under mild conditions so as to differentiate between liquefaction properties. Favourable conversions and liquid yields were obtained. The «screening» procedure was devised after a number of preliminary tests and shown to be consistent by total mass and sulphur balances. The highest liquid selectivity was observed with Beypazarı and the «lightest» liquid with Elbistan. However, the liquids derived were of high sulphur.

In the next stage, samples from other substantial deposits will be subjected to the standard screening test, qualitative and quantitative relationships between lignite properties and liquefaction performance will be sought, and three or four samples will be selected for more detailed autoclave experiments.

ADDENDUM

Experiments of total mass and sulphur balances

For total mass and sulphur balances additional determinations are made, viz. product gas is collected and characterized, and water recovered as mixture with THF in evaporation is quantified.

The gas is bubbled through two absorbers containing excess 2N sodium hydroxide and the sweet gas is collected over water. Gas volume is measured as displaced water. Gas density is determined by the method of Regnault (Yarzab et al., 1980).

The contents of the absorbers are combined. Absorbed carbon dioxide is determined by acidification followed by absorption in soda-asbestos (Given and Yarzab, 1978). Trapped hydrogen sulphide is determined by wet oxidation and subsequent precipitation as barium sulphate.

Water carried over with THF in evaporation is estimated chromatographically in a 2.5 m x 1/8" Porapak Q column with TCD detection (Guin et al., 1977).

Quantity of input hydrogen is calculated by the ideal gas law.

REFERENCES

ASTM D 197-30, 1980 Annual book of ASTM stds., 26, 199.

ASTM D 1756-62, ibid, 264.

ASTM D 2015-77, ibid, 307.

Bayraktar, K.N., 1981, Studies on the processing and utilization of two Turkish lignites: Ph. D. thesis, The University of Birmingham, 273.

————and Özkaplan, O., 1982, Kömür sıvılaştırma literatür çalışması: MTA Publ., 88, Ankara.

BS 1016, Part 11, 1969, 13.

Charlesworth, J.M., 1980, Influence of temperature on the hydrogenation of Australian Loy-yang brown coal 1. Oxygen removal from coal and product distribution; Fuel 59, 859-864.

Cudmore, J.F., 1977/78, Noncatalytic hydrogenetion of Australian coals; Fuel processing technology, 1, 227-241.

Curran, G.P.; Struck, R.T. and Gorin, E., 1967, Transfer process to coal and coal extract, IEC proc. des. dev., 6, 166-173.

Given, P.H. and Yarzab, R.F., 1978, Structure of coal and coal products: Karr., Jr. C., ed., Analytical methods for coal and coalproducts, vol. 2, Academic Press, New York, 3-39.

Gorin, E., 1981, Fundementals of coal liquefaction: Elliot, M.A.,ed., Chemistry of coal utilization-second supplementary volume, New York, 1845-1918.

Guin, J.A.; Tarrer, A.R.; Pitts, W.S. and Prather, J.W., 1977, Kinetics and solubility of hydrogen in coal reactions, Ellington, R.T., ed., Liquid fuels from coal, Academic Press, New York, 133-152.

Kamiya, Y.; Sato, H. and Yao, T., 1978, Effect of phenolic compounds on liquefaction of coal in presence of hydrogen donor solvent: Fuel, 57, 681-685.

Montgomery, W.J., 1978, Standard laboratory test methods for coal and coke, Karr, Jr., C., ed., Analytical methods for and coal products, vol. 1, Academic Press, New York, 191-246.

Morita, M.; Sato, S. and Haşimoto, T., 1979, Effect of hydrogen pressure on rate of direct coal liquefaction: ACS div. fuel chem. pr., 24, 2, 270-279.

MTA Genel Müdürlüğü, 1983, Türkiye'nin bilinen linyit, taşkömür ve asfaltit kaynakları: MTA Publ., Ankara.

Neavel, R.C., 1976, Liquefaction of coal in hydrogen-donor and non-donor vechiles: Fuel, 55, 237-242.

Pastor, G.R.; Angelovich, J.M. and Silver, H.F., 1970, Study of the interaction of solvent and catalyst in coal hydrogenation: IEC proc. des dev., 9, 609-611.

Ruether, J.A., 1977, Kinetics of heterogeneously catalyzed coal hydroliquefaction, IEC proc. des. dev., 16, 249-253.

TÜBİTAK TBAG 575-B project interim repts no 1 and 2, 1984, Ankara, 27 and 30.

Turkish Standard 362, 1966, 4

Turkish Standard 363, 1966, 5

Turkish Standard 711, 1969, 5

Turkish Standard 1042, 1971, 2

Turkish Standard 1044, 1971, 3

Turkish Standard 1051, 1972, 3

Whitehurst, D.D.; Mitchell, T.O. and Farcasiu, M., 1980, Coal liquefaction: Academic Press, New York, 378.

Yarzab, R.F.; Given, P.H.; Spackman, W. and Davis, A., 1980, Dependence of coal liquefaction behaviour on coal characteristics: Fuel, 59, 81-92.

PSEUDOLEUCITE FROM HAMİTKÖY AREA, KAMAN, KIRŞEHİR OCCURRENCE AND ITS USE AS A PRESSURE INDICATOR

A. Taylan LÜNEL* and Orhan AKIMAN*

ABSTRACT.— Kırşehir batholith outcropping over a large area in Central Anatolia consists mainly of coarse grained felsic igneous rocks. Around Hamitköy area the batholith seems to be syenitic in composition and is cut by silica deficient feldspathoid bearing microsyenitic dykes striking along E-W and NE-SW directions. Pseudoleucite occurs as large phenocrysts, however it is optically discontinuous and consists of discrete leucite crystals. Minor amounts of sericite and smectite are observed as alteration products of the pseudoleucite. Chemical analyses display the fact that Hamitköy pseudoleucites resemble to leucites, with their small amount of Na_2O content, and to pseudoleucites in their total alkali deficiency. Phase study diagrams of the residue system suggest that the crystallization of pseudoleucite is a pressure sensitive phenomenon and that it may be possible to use the presence of pseudoleucite as a pressure indicator. It is tentatively suggested here by the authors that pseudoleucite forms from a volatile-rich, silica poor magma under approximately 2 kbars of pressure, which corresponds to a depth of approximately 7 kilometers in the crust.

INTRODUCTION

The results of chemical and mineralogical study of pseudoleucites obtained from microsyenite dykes of Hamitköy area, Kaman are presented in this paper.

Kırşehir crystalline massif as named by several authors (Arni, 1938; Bailey and McCallien, 1950; Egeran and Lahn, 1951; Ketin, 1953 and Seymen, 1982) consists of metamorphic basement rocks which are intruded by a heterogeneous batholith. Felsic intrusive rocks of the western part of the batholith around Kaman area were mapped by various workers (Baykal, 1941; Buchardt, 1956 and Seymen, 1982) and granitic, aplitic, grdnodioritic, monzonitic, syenitic and dioritic rock types were observed. The rocks of the metamorphic basement were studied in detail by Erkan (1975) and Seymen (1982) and were named as "Kaman Group" by Seymen.

Arni and Schroeder (1938) mentioned about leucite porphyry dykes around Kaman area. Intrusive rocks of Kaman region were named as Baranadağ and Buzlukdağ plutons by Seymen (1982) and he further mentioned that Baranadağ pluton consisted of quartz-diorite, granodiorite and quartz-monzonite, while Buzlukdağ pluton was mainly consisted of syenite, nepheline syenite, leucite syenite, trachyte and phonolite.

Age of the intrusive rocks of Kaman region is suggested to be of Eocene (Ayan, 1963), Paleocene (Ketin, 1963; Seymen, 1982) or Upper Cretaceous (Ataman, 1972).

The felsic intrusive rocks of Kaman-Keskin area constitute the northwestern part of the large Kırşehir batholith. There appears to be a rough zoning where outer parts consist mainly of oversaturated quartz-rich granitic rocks while in central parts occur saturated and silica deficient feldspathoid bearing syenitic rocks (Fig. 1) (Baykal, 1966 and Ketin, 1962, 1963).

The syenitic parts of the batholith around Kaman area are well known for their distinctive suite of potassium-rich pseudoleucite bearing microsyenitic dykes. They occur as a group of simple and composite dykes striking along E-W and NE-SW direction intruding both syenite and gabbroic

rocks which are probably roof pendants of the batholith (Fig. 2). The dykes range in composition from amphibole phonolites, augite-biotite phonolites to a few syenite porphyries and late quartz porphyries. Some dykes are composite, with borders, consisting of mafic hornblende phonolite while central parts consist of leucocratic biotite phonolite. The thickness of the dykes range from few cm's to several 10's of meters.

The fractures into which the dykes were emplaced, were formed later than the intrusion of the syenite batholith. Many dykes show fine grained chilled margins. Phenocrysts of hornblende and feldspar, within the border zone, show parallel alignment to the walls of the dykes, which is presumably due to internal friction that developed during the flow of relatively viscous magma within the fracture.

MINERALOGY

Pseudoleucite occurs as large phenocrysts set in a fine to medium-grained groundmass (Plate I A). Size of the crystals range from 1 cm upto 15 cm in diameter. In altered upper parts of the dykes the pseudoleucite crystals are easily extracted from the groundmass.

Microscopically, optically discontinuous pseudoleucite phenocrysts display a well developed zoned structure. The contact between the phenocrysts and groundmass is sharp. In the border zone of the crystals there occurs a cryptocrystalline region of few mm's thickness. Next to the border zone, in the columnar crystalline part, elongated leucite crystals occur with their long axis perpendicular to the border zone. The thickness of this zone is upto 0.5 cm. The central part of the phenocrysts consist of coarse grained, unoriented, optically discontinuous mosaic of leucite crystals which sometimes display pseudo-graphic texture (Plate I B).

Sericite occurs as an alteration product of leucite. In the phenocryst, sericitization generally starts along the crystal boundaries and works its way to the centre of the leucite crystals. In extreme cases of alteration sericite replaces the entire phenocryst and produces secondary pseudomorphs of leucite.

X-ray diffractograms (Fig. 3) show also the presence of leucite and sericite-muscovite. There are two spurious peaks which are probably of leucite, occuring at 6.51 A° and 2.17 A° d-spacing. Samples prepared for clay analysis indicated the presence of minor amount of smectite.

COMPOSITION

Leucite is a highly characteristic igneous mineral that forms from potassium-rich, silica-poor magmas which solidify in extrusive and hypabyssal environment, it is not reported from deep seated plutonic rocks. Psedoleucite, on the other hand, is an aggregate of crystals consisting of potassium feldspar, nepheline and minor quantities of sodalite, cancrinite or a zeolite, that shows the crystal habit of leucite and occurs in both plutonic and volcanic rocks (Deer et al., 1965).

Leucite analyses generally conform the ideal formula $KAlSi_2O6$, where Si: Al ratio is very close to 2:1. Total alkalies ion-number on the basis of 6 oxygens approximates closely to 1.00. Only a limited amount (upto 13 %) of Na^+ substitution of K+ occurs. However, pseudoleucite analyses published in «Rock Forming Minerals (v.4, Table 34, p. 282)» of Deer, Howie and Zussman (1965), show that there are substantial amounts of Na^+ substituting K^+ and the total alkalies ion-number on the basis of 6 oxygens ranges from 0.68 to 0.93, which clearly indicates a striking alkali deficiency.
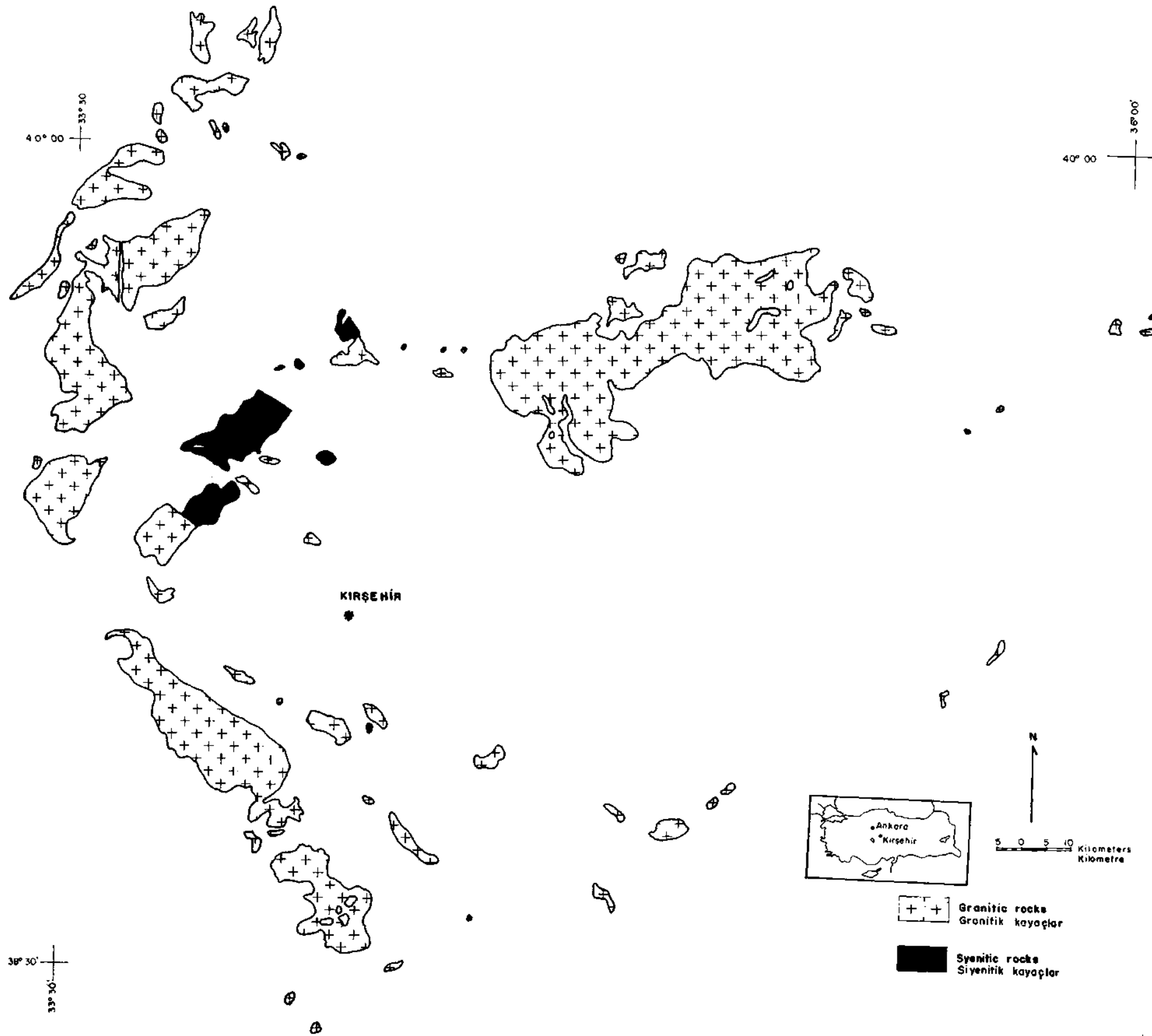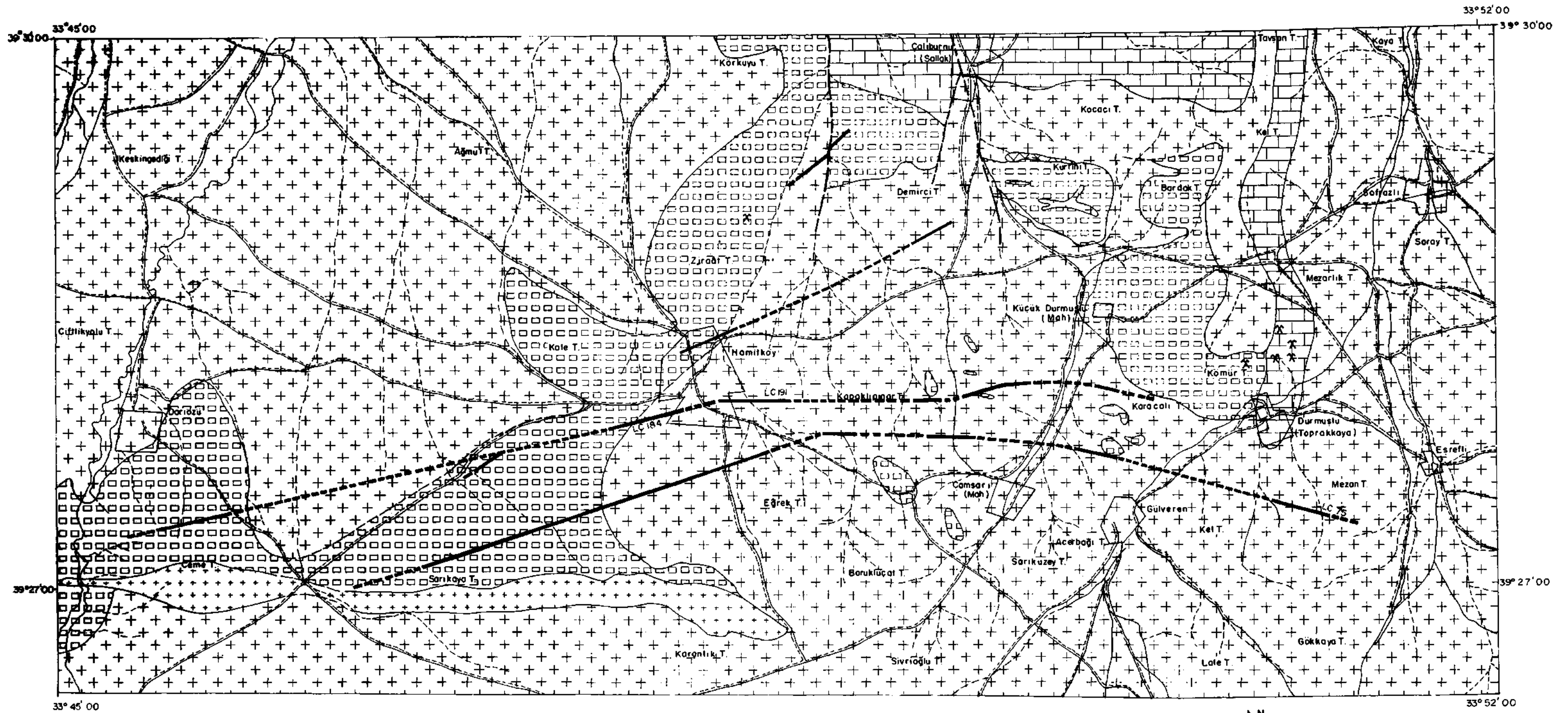
Fig. 1 - Schematic geological map of the Kırşehir batholith (from the Kayseri, Sinop and Sivas sheet, Geological Map of Turkey; Ketin, 1962, 1963 and Baykal, 1966).

33°45'00 33°52'00
39°30'00 39°30'00

Körkuyu T. Çalıburnu (Sallak) Tavşan T. Koya T.

Kocacı T. Kel T.

Ağmu T. Kırmır Bardak T. Softazlı

Demirci T. Saray T.

Zıraat T. Mezarlık T.

Küçük Durmuşlu (Mah.)

Çiftlikoglu T. Kale T. Hamitköy Kömür T.

LC 191 Kapaklıqapar T. Karaçalı T.

Darıözü LC 184 Durmuşlu (Toprakkaya)

Esrefli

Camsar (Mah.) Mezan T.

Egrek T. Gülveren LC 75

Acerbağı T. Kel T.

Sarıkuzey T.

Çeme Sarıkaya T. Borukluçat T.

39°27'00 39°27'00

Karanlık T. Sivrioğlu Lale T.

Gökkaya T.

33°45'00 33°52'00

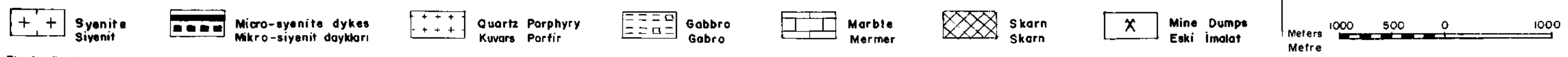| | Syenite Siyenit | | Micro-syenite dykes Mikro-siyenit daykları | | Quartz Porphyry Kuvars Porfir | | Gabbro Gabro | | Marble Mermer | | Skarn Skarn | | Mine Dumps Eski İmalat |

N

Meters 1000 500 0 1000
Metre

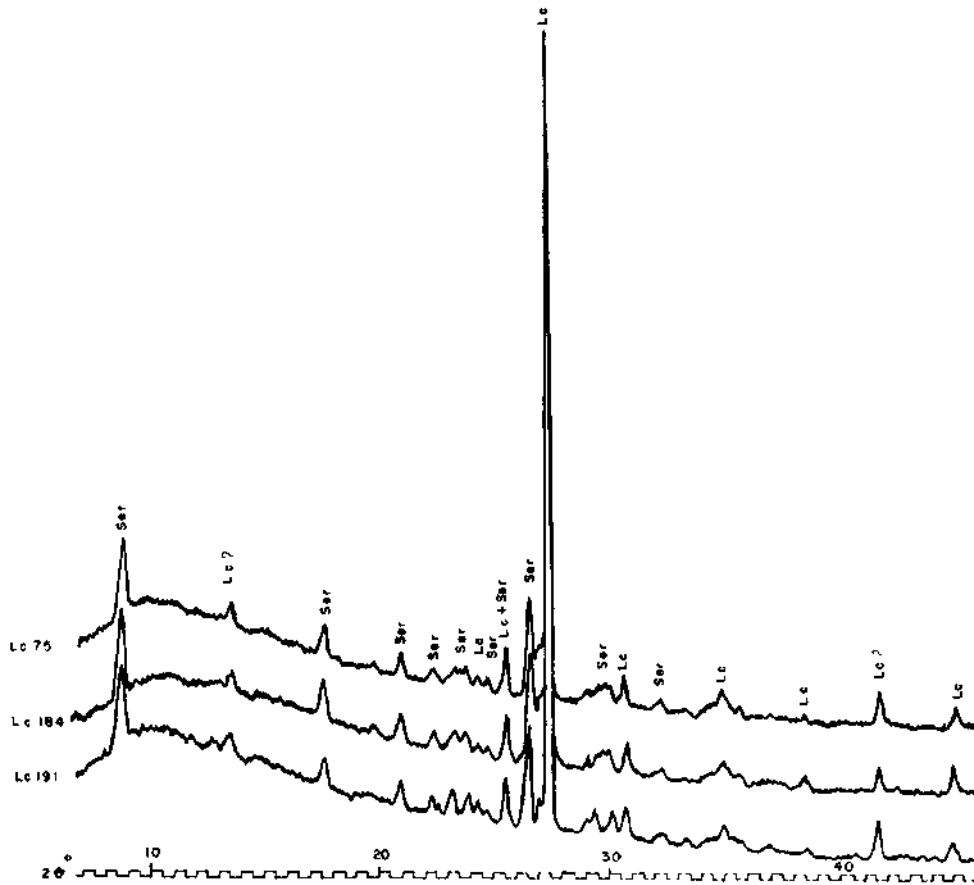Fig. 2 - Detailed geological map of Hamitköy area, Kaman, Kırşehir (mapped by O. Akıman, on 1:25 000 scale).

Fig. 3 - X-ray diffractograms of psedoleucite from Hamitköy. Cu-tube radiation, Ni-filter; 40 kV, 22 mA; Slits D 2°,R 0.1, S 1/2°; 4x10³ .CPS;TC 2.

Chemical analyses of three pseudoleucites from two different dykes, from Hamitköy area (Fig. 2) are given in Table 1. Comparing, present analyses with that of Deer, Howie and Zussman (1965) indicates that Hamitköy pseudoleucites are similar to leucites in that there is a very limited Na^+ substitution in their bulk composition whereas they resemble to pseudoleucites in the deficiency of their total alkali content.

Chemical analyses of pseudoleucites and leucites are plotted in a SiO_2-$NaAlSiO4$-$KAlSiO_4$ triangular diagram (Gittings, 1979), where phase equilibria for P=1 atm; PH_2O= 1 kbar, 2 kbar and 5 kbar (Schairer and Bowen, 1935; Schairer, 1950; Hamilton and MacKenzie, 1965; Taylor and MacKenzie, 1975; Morse, 1969; Roux and Hamilton, 1976) are also shown (Fig. 4). There is a very striking coincidence of location of pseudoleucite analyses of P_1, P_2, P_3 and P_5 with that of cotectic curve between Na-K feldspar and leucite field, for P=2 kbar. This probably suggests that the crystallization of pseudoleucite is a pressure sensitive phenomenon and that it is possible to use the presence of pseudoleucite as a pressure indicator. The plotting of points towards the low temperature-end along the cotectic probably indicates the control of temperature where Hamitköy pseudoleucite crystallizing at higher temperatures than Cnoc-na Sroine (P_3) pseudoleucite (Shand, 1910).

Table 1 - Chemical analyses of pseudoleucites from Hamitköy, Kaman

	Lc 75	Lc 184	Lc 191	Lc HK
SiO_2	58.720	59.330	59.480	59.180
TiO_2	0.040	0.040	0.033	0.038
Al_2O_3	23.870	24.010	24.150	24.010
FeO	0.540	0.520	0.690	0.580
MnO	0.008	0.006	0.011	0.008
MgO	0.130	0.040	0.050	0.070
CaO	0.130	0.080	0.080	0.100
Na_2O	0.240	0.260	0.300	0.270
K_2O	14.200	14.630	14.430	14.420
P_2O_5	0.013	0.011	0.010	0.011
A.K. (LOI)	1.760	1.920	1.630	1.770
Toplam (Total)	99.651	100.847	100.864	100.457

Number of ions on the basis of 6 oxygens

	Lc 75		Lc 184		Lc 191		Lc HK	
Si	2.075		2.078		2.076		2.076	
Al	0.994		0.991		0.993		0.993	
Ti	0.001		0.001		0.001		0.001	
Fe^{2+}	0.016	1.023	0.015	1.012	0.020	1.020	0.017	1.019
Mg	0.007		0.002		0.003		0.004	
Ca	0.005		0.003		0.003		0.004	
Na	0.016	0.656	0.018	0.672	0.020	0.662	0.018	0.663
K	0.640		0.654		0.642		0.645	

Partial CIPW norms

	Lc 75	Lc 184	Lc 191	Lc HK
q	44.56	43.87	44.31	44.27
kp	54.19	54.81	54.15	54.34
ne	1.25	1.32	1.54	1.39

Analyst: A.T. Lünel; LOI by A. Uyankaya.

Plotting of leucite analyses L_{1-7} (Deer et al., 1965) on the same diagram (Fig. 4) shows an interesting trend which is parallel to the cotectic curve between orthorhombic (K, Na) $AlSiO_4$ solid solutions—(Na, K) nepheline and leucite fields, for P=1 kbar; but somewhat shifted to SiO_2-rich regions. This shift probably reflects a somewhat different PH_2O conditions and that leucite crystallization is also presumably a pressure controlled process. Pseudoleucite (P_4) from Bearpaw Mountains (Zies and Chayes, 1960) plots along the leucite trend and probably more closely related to leucites in its origin.

Chemical analyses of pseudoleucites and leucites are also plotted in a SiO_2-K_2O-Al_2O_3 triangular diagram (Deer et al., 1965), where phase equilibrium for P=1 atm (Schairer and Bowen, 1955) is shown. Location of the points indicate a striking trend which is linearly aligned and roughly parallel to the K-feldspar-leucite cotectic curve which may support the above conclusions (Fig. 5).
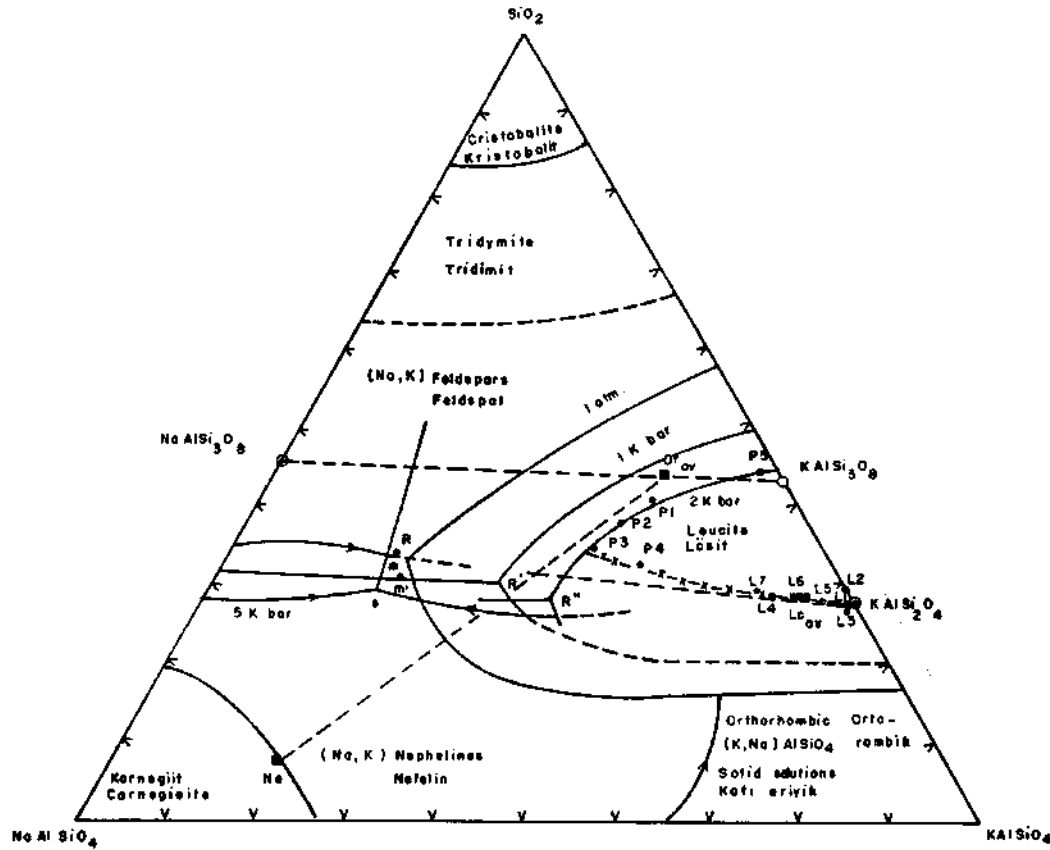
Fig. 4 - Phase equilibrium diagram of the system NaAlSiO₄-KAlSiO₄-SiO2-H₂O for P= 1 atm, PH₂O = 1 kbar, 2 kbar,

5 kbar (Deer et al., 1965; Gittings, 1979). R=Reaction point and m=Ternary minimum at 1 atm, R' and m' at 1 kbar, R" at 2 kbar; e=Ternary eutectic (undersaturated portion of the system); P₁₋₄: Pseudoleucite analyses from Deer et al. (1965, v. 4, p. 282), P₅: Average of Hamitköy pseudoleucites; L₁₋₇ : Leucite analyses from Deer et al. (1965, v. 4, p. 280); Ne: Morozewicz nepheline composition; Lc_va :Average composition of leucites; Or_av : Average composition of potassiu mfeldspars.

CONCLUSION

Pseudoleucites obtained from microsyenite dykes of Hamitköy area are unique in their mineralogy and composition. In other natural rocks, pseudoleucites are generally described as an association of nepheline and alkali feldspar. Thus indicating an ion exchange phenomenon where potassium-rich magma initially crystallized potassic leucite that later changed into more sodic type with falling temperature. Subsequent cooling caused exsolution of nepheline and alkali feldspar where leucite structure is destroyed but retaining leucite crystal morphology (Gittings, 1979). However, in Hamitköy pseudoleucites, leucite is the dominant phase and nepheline occur only in very minor quantities, which probably indicates a higher temperature of crystallization that did not permit Na+ substitution. Chemically, Hamitköy pseudoleucite plot very close to potash-feldspar composition and is far removed from the positions of other pseudoleucites (P₁₋₄) and leucites L(1-7) (Fig. 4).
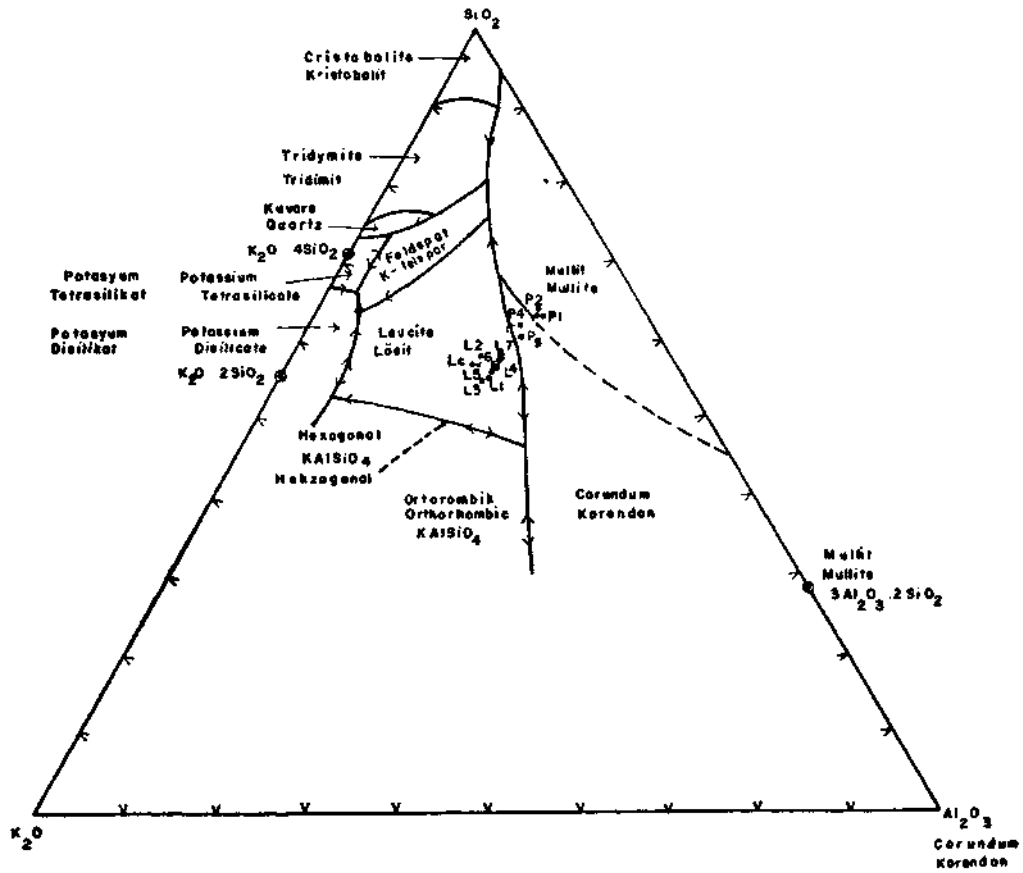
Fig. 5 - Phase diagram of the system $K_2O-Al_2O_3-SiO_2$ (after Schairer and Bowen, 1955, from Deer et al., 1965). P- Pseudoleucites; L- Leucites (as explained in Fig. 4).

The presence of pseudoleucite in igneous rocks may be used to indicate the pressure conditions prevailed during the formation of the phenocrysts. Although this should be proved by further experimental work at high pressure, it is tentatively suggested here that approximately a pressure of 2 kbars, which corresponds to a depth of approximately 7 kilometers (Barker, 1983) is necessary for formation of pseudoleucite in a volatile-rich undersaturated magma. This conclusion is also in agreement with the field observations in that leucite or pseudoleucite occur mainly as phenocrysts in volcanic or hypabyssal rocks but rare or absent in deepseated plutonic environment.

REFERENCES

Arni, P., 1938, Kırşehir, Keskin ve Yerköy arasındaki havalide vukua gelen zelzele: MTA Publ., B, 1, 18 p., Ankara.

————and Schroeder, A., 1938, Kırşehir şimali garbisinde bulunan Kortundağı-Baranadağı granitindeki lösit porfir damarları: MTA Rep., 825 (unpublished), Ankara.

PLATE

PLATE - 1

A - Photograph of Hamitköy pseudoleucite (Lc 75), Mag. 1/2.

B - Photomicrograph of Hamitköy pseudoleucite (Lc 184), displaying mosaic of leucite crystals and pseudographic texture, Mag. X 40, Polarised light.
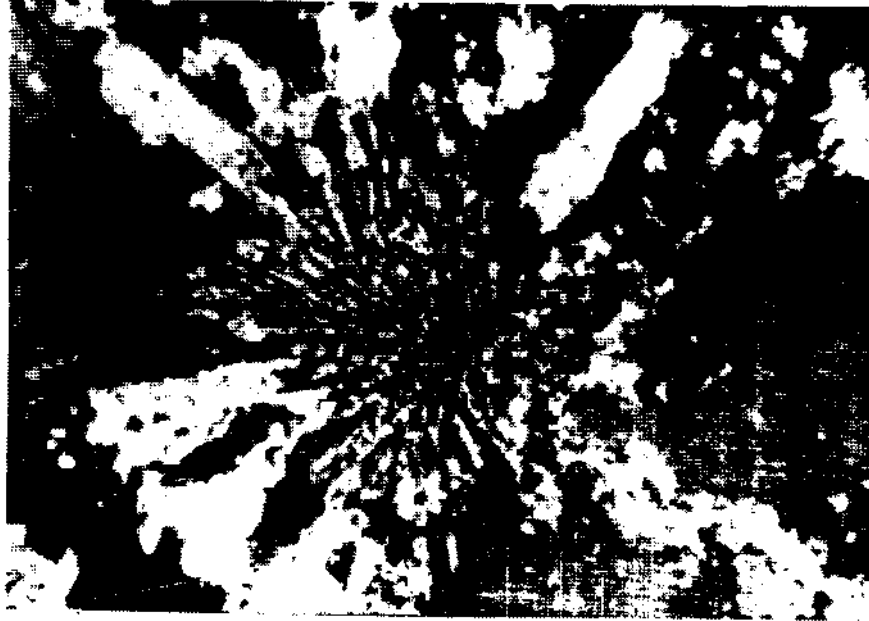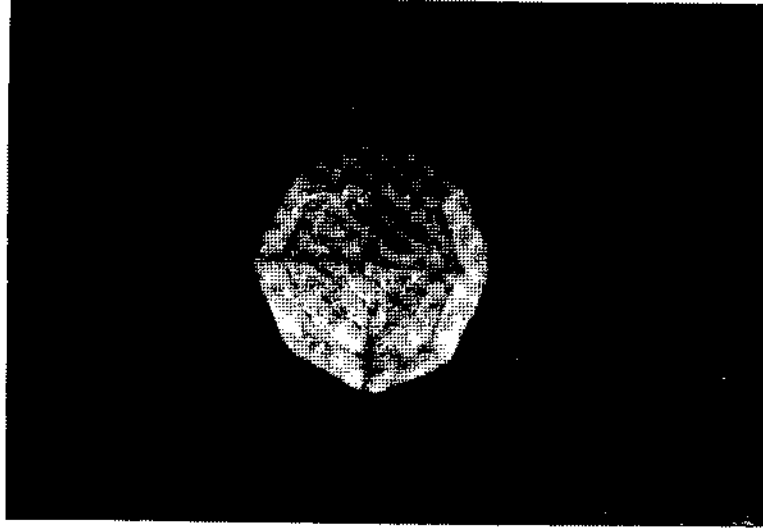
Ataman, G., 1972, Ankara'nın güneydoğusundaki granitik-granodiyoritik kütlelerden Cefalık dağın radyometrik yaşı hakkında on çalışma: Hacettepe Fen ve Müh. Bilimleri Dergisi, 2, 1,   44-49, Ankara.

Ayan, M., 1963, Contribution a l'etude petrographique et geologique de la region situee au Nord-Est de Kaman (Turquie): MTA Publ., 115, 332 p, Ankara.

Bailey, E.B. and McCallien, W.J., 1950, The Ankara Melange and the Anatolian thrust: MTA Bull., 13, 40, 17-21.

Barker,   D.S., 1983, Igneous rocks: Prentice-Hall, Inc., Englewood Cliffs, New Jersey, 417 p.

Baykal, F., 1941, Kırıkkale-Kalecik ve Keskin-Bala mıntıkalarındaki jeolojik etütler: MTA Rep., 1448 (unpublished), Ankara.

————, 1966, Explanatory text of the Geological Map of Turkey (1:500 000) Sivas sheet: MTA Publ., Ankara.

Buchardt, W.S., 1956, Orta Anadolu'da 1:100 000 ölçekli jeolojik harita çalışmaları hakkında rapor: MTA   Rep., 2675, part I, (unpublished), Ankara.

Deer, W.A.; Howie, R.A. and Zussman, J., 1965, Rock Forming Minerals: Longmans, London.

Egeran, N. and Lahn, E., 1951, Note on the tectonic position of the northern and central Anatolia: MTA Bull., 41, 23-27, Ankara.

Erkan, Y., 1975, Orta Anadolu masifinin Kırşehir bölgesinde etkili rejyonal metamorfizmanın petrolojik incelenmesi: Hacettepe Univ. Doçentlik Tezi (unpublished), Ankara.

Gittings, J., 1979, The feldspathoidal alkaline rocks; in The evolution of the igneous rocks: Yoder, H.S. Jr., ed., Princeton Univ. Press New Jersey.

Hamilton, D.L. and MacKenzie, W.S., 1965, Phase equilibrium studies in the system NaAlSiO4-KAlSiO4-SiO2-H_2O: Min. Mag., 34, 214-231.

Ketin, İ., 1953, Yozgat, bölgesinin jeolojik lövesi hakkında memuar: MTA Rep., 2141, 50 (unbuplished), Ankara.

————, 1962, Explanatory text of the Geological Map of Turkey (1:500 000) Sinop sheet: MTA Publ., Ankara.

————, 1963, Explanatory text of the Geological Map of Turkey (1:500 000) Kayseri sheet: MTA Publ., Ankara.

Morse, S.A., 1969, Syenites: Ann. Rep. Dir. Geophys. Lab., 67,   112-120, Washington,

Roux, J. and Hamilton, D.L., 1976, Primary igneous analcite: An experimental study, Jour. Pet., 17, 244-257.

Schairer, J.F., 1950, The alkali-feldspar join in the system NaAlSiO$_4$-KAlSiO$_4$-SiO$_2$: Jour. Geol., 58, 512-517.

————and Bowen, N.L., 1935, Preliminary report on equilibrium relations between feldspathoids, alkali-feldspars and silica: Trans. Amer. Geophys. Union 16th Ann. Meeting, Nat. Res. Council, Washington, D.C.

————and————, 1955, The system K$_2$O-Al$_2$O$_3$-SiO$_2$: Amer. Jour. Sci., 253, 681.

Shand, S.J., 1910, On borolanite and its associates in Assynt: Trans. Edin. Geol. Soc., 9,   376.

Seymen, İ., 1982, Kaman dolayında Kırşehir masifinin jeolojisi: İstanbul Tek. Univ. Maden Fak., Do9entlik Tezi, 164   (unpublished).

Taylor, D. and MacKenzie, W.S., 1975, A contribution to the pseudoleucite problem: Contr. Mineral. Petrol., 49,   321-333.

Zies, E.G. and Chayes, F., 1960, Pseudoleucites in a tinguaite from the Bearpaw Mountains: Jour. Pet., 1,   86.

FULGURITE AT THE MEZARGEDİĞİ AREA İZMİR-SELÇUK-ÇAMLIK VILLAGE, TURKEY

Hasan DURGUN* and İsmail Hakkı KARAMANDERESİ*

ABSTRACT.— Fulgurite in the Çamlık Region is a black silica glass with the white spherulitic inclusions. Those feldspar-like inclusions are lath shaped grains and composed of nonreactive SiO2-modifications such as tridymite, cristobalite, lechatelierite, coesite, and quartz. The silica glass is the melting product of a high quartz bearing silicate rock and quartzose sand. In the area the origional materials are quartz veinlets bearing muscovite schist and quartzose sand used in concrete base fastening the power-line pole. Persistent melting of the mother-lode has increased the amount of the melt. Hence flow of the liquid material has taken place for a while within few meters. Because of the flow migration from the generating environment the produced silica glass has spreaded out around and scattered within 25 square meters. Solid product shows hollow tubes along the flow channels. The steam and reaction gases have given vesicular cavities in the solidified front. These vesicular structures have given a spongy structure to the solid glassy mass. The white angular granules in the black glassy matrix have been identified as the SiO2-modifications of the quartz in thin sections under the microscope.

INTRODUCTION

A press news informed that after lightning upon an area around Çamlık village petroleum has been found (Bulvar Jan. 14th, Hürriyet Jan. 16th, Yeni Asır Jan. 25th). This press information has remined us about the probability of the fulgurite formation. The occurance has been checked in the field and studied macroscopically and microscopically.

The obsidian-like silica glass has been formed at the foot of a high power-line pole. It is an accumulation of a silisified rock melt that shows flow structure. The mode of formation is not as it has been commended but because of the electric arc from the power-line released from the isolation porcelain pot on top of the iron pole (Fig. 1). The electric current has passed through the iron-pole to the ground, and during this current jump an arc has been sreated at the contact with the ground. The tremendous heat of this arc has melted quartz and quartz bearing muscovite schist and given silica glass; fulgurite.

GENERAL GEOLOGY

The stratigraphic succession starts with the muscovite schist which has been enveloping the augen gneiss nucleus. These metamorphic units belong to the Menderes Massif of the Western Anatolia. Marble and crystallized limestone follow up. Serpentinites in the succession are emplaced tectonically. Then Neogene elastics, clays and marls, and marly limestones cover some depresions. Pliocene terraces and quaternary alluvial deposits are the latest placers (Fig. 3).

The stratigraphic unit in the fulgurite bearing location is muscovite schist. The mineral constituents are muscovite, quartz, feldspars (especially Na-plagioclases), and chlorite. Opaque minerals are the iron oxide constituents. They are accessery minerals.
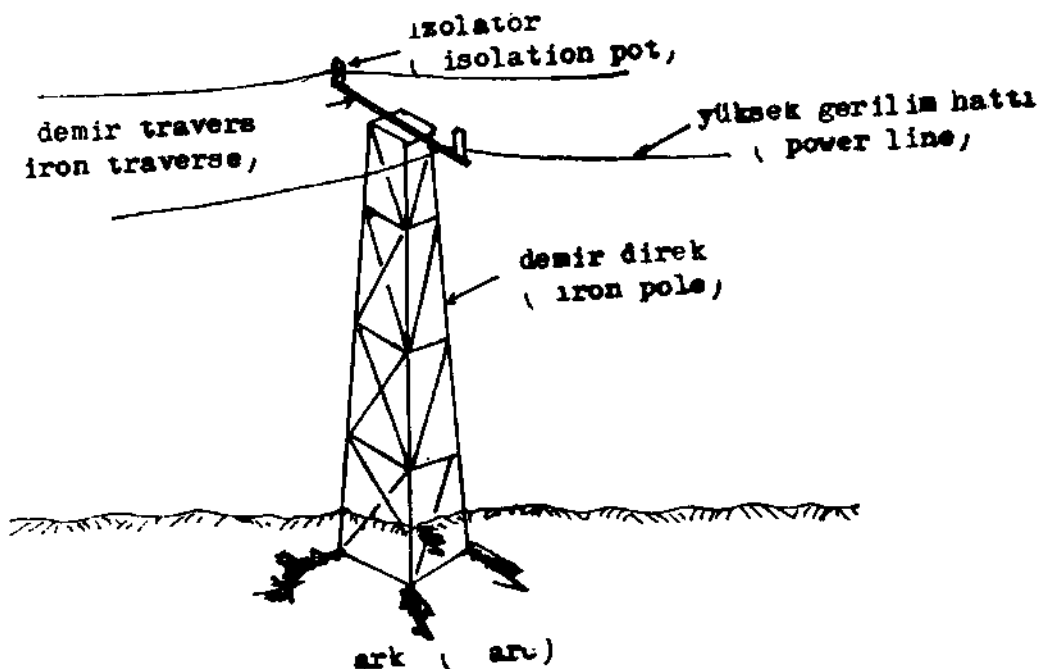
Fig. 1 - Current flow to the ground through the iron pole, and formation of the arc-light.

Faulting is the main tectonic unit in the area (Fig. 3). Structural appearance have been shaped by the block movement in trusts and gravity faults. The East-West and/or near-by striking lineations are the basic features. Those lineations mark the characteristic direction of the Alpine tectonic units.

Fold structures are very poor and they are the results of trusting and gravity faults. Plastic flow structures seem to be drag folds.

FULGURITE AND ITS MODE OF FORMATION

The generated glassy material formed at the base of a high voltage power-line pole shows flow structure. The pole is made up of iron, and hence it is a conductive body, Photo 1. Silica glass has been spreaded out within 25 square meters. From the four feet of the iron-pole the melt radially flows out (Fig. 1) and (Photo 1). Along the flow channels hollow tubes of the glassy material have been formed Photo 2. The diameter of the tubes have been changing up to 20 centimeters. At the exposed extend of those tubes the flowing melt accumulated and this liquid mass has traveled for a while and solidified Photo 1. The exposed surface of the glassy mass shows spongy structure due to the vesicular cavities.

The glassy mass is in brillant black colour at the surface. When the hollow tubular pipes are examined in section one can see the inside face has been glazed and shows a pearly appearance. It is dark gray in colour. Behind the glaze there is a porous zone having a spongy structure. The thick-ness of this zone is few centimeters. It is gray in colour, and consists of angular grains in glassy matrix. Those grains are similar, in appearance, to feldspars and are presenting a gosh structure. But in spite of these similarities in appearance and structures the microscopic identification presents spherulite

composition having SiO_2-modifications such as tridymite, cristobalite, coesite, lechatelierite, and quartz.

The second zone in section shows obsidian-like lithology. It is dense and compact, and fracturing conchoidally.
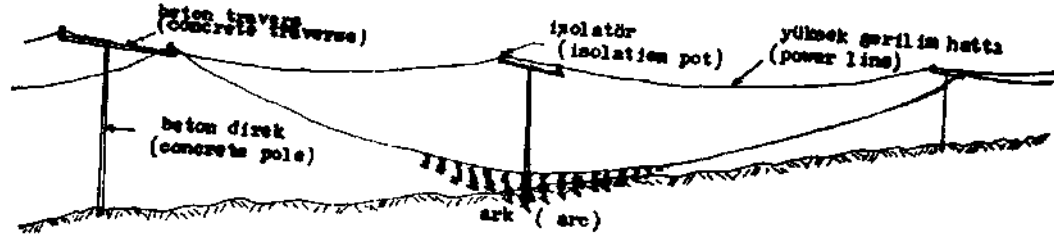

Fig. 2 – Current jump to the ground, and formation of the arc-light.

The third zone is gray in colour and has feldspars-like white spherulite grains. The vesicular cavities in this layer are small, and due to this vesicularity there is a spongy structure.

The outer surface of those tubular pipes carries the rock fragments and chips of the muscovite schist and concrete materials.

The obsidian-like dense rock has a moderate specific gravity, but specimens having spongy structure are quite light. The specific gravity of the rock changes from 1.75 to 2.75 gr/cm^3.

Photo 1 – The iron pole of the high voltage power-line. The glassy materil having flow structure has been formed at the four feet and is radially lining out to the surface.
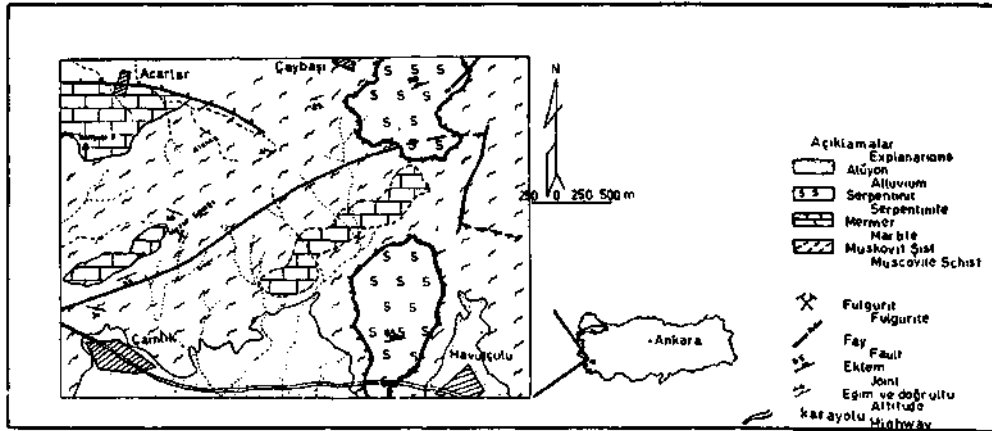
Fig. 3 - Geology of the Çamlık Region.

THE PROCESS CREATED THE FULGURITE

The formation of the fulgurite has taken place at the base of a high voltage power-line pole, Fig. 1. It is an iron pole, hence conductive. The energy has been taken from the high voltage power-line through the iron pole. The releasing of the power-line from the isolation pot on top of the pole yielded a connection with the conductive iron pole. The electric current flowing into the ground through the pole has created an arc at the feet, Fig. 1. The tremendous heat of this arc has melted the quartz muscovite and quartzose sand of the concrete basement. This liquidified melt has flowed through the channels and formed the hollow tubular fulgurite, Photo 2. The heat generation from the arc is more or less same as it has been in Plasma Technique in metal extraction in this method the heat may be maintained up to 16 000°C. The persistency of the heat has caused the increase of the melt in amount by feeding of a continuous melting. The melt which comes out in this way has flowed for a while and solidified in a distance. The reason of the change of the state is not a lightning action as it has been recommended by some scientists and peasants. If it would be formed due to a lightning action the fulgurite formation would show a line segment or a point location. On the contrary here it shows a migration and flow structure. The lightning action may create only an in situ product, and the amount of the melt can not be as much as in this particular case. The same formation has been studied in the North of Yozgat in 1974. In this area, too, the silica glass was identified along a line segment between two high voltage power-line poles, Fig. 2. It was an in situ formation and explained in the same way.

CONCLUSION

The silica glass which is studied in the field has been formed by the electric arc. This arc has been produced by a high voltage power-line passing along the field. The realesing of the power-line from the isolation pot on top of the pole has been loosened the wire and it has come contact with the iron pole. The current has started to flow to the ground through the iron pole. At the foot of the pole the electric charge created an arc which may usually produce a heat with an extremely high temperature over 2000°C. This high temperature heat has melted the quartz sand and quartz bearing muscovite schist. This change of state has graded into fulgurite formation.
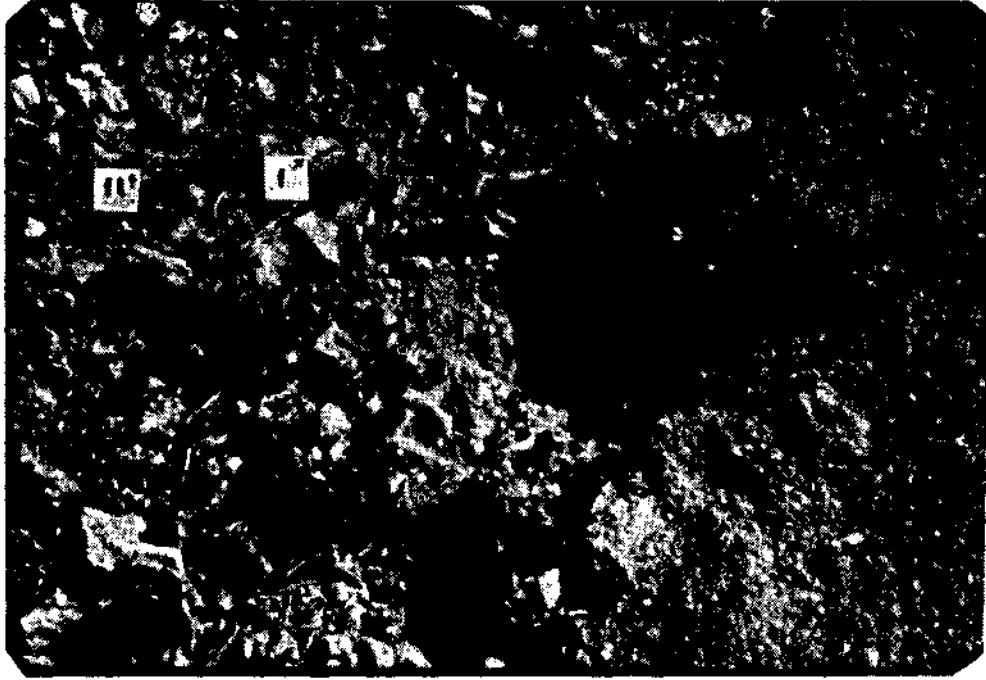
Photo 2 - Tubular fulgurite formation. The hollow nearby the hammer is the channel of the tubular
pipe. f - glazed face of the tube; f1 - flow structure on the fulgurite.

Fulgurite, in Çamlık Region, has a black colour. It is pearly and shows conchoidal fracture.
The vesicular structure is due to the reaction gases and steam generated from the ground water.
The hollow tubular structures along the channels are remarkably formed. These tubular pipes
have the diameters up to 20 centimeters.

Manuscript received May 6, 1955

REFERENCES

American Geological Institute, 1957, Dictionary of Geological Terms: Dolphin Books, Doubleday and Company, Inc.
    Garden City, N.Y. Third ed., 1962, pp. 197.

Bulvar Gazetesi, Jan. 14 , 1985, Press, pp. 1, İstanbul.

Hürriyet Gazetesi, Jan. 16th , 1985, Press, pp. 3, İstanbul.

Kerr, P.F., 1959, Optical Mineralogy: McGraw-Hill Book Company, Inc. N.Y. Toronto London. Third ed.
    pp. 247-248.

Keskin, B., 1972, Kuşadası-Germencik-Aydın Arası Büyük Menderes Grabeninin Jeotermal Değerlendirilmesi Hakkında
    Jeolojik Rapor: MTA Ege Böl. Md., J.E./14 (Unpublished) Bornova.

Yeni Asır Gazetesi, Jan. 25 , 1985, Press, pp. 1. İzmir.

SEISMIC REFLECTION STUDIES IN POLATLI REGION, TURKEY

M. Işık TURGAY* and Cengiz KURTULUŞ*

ABSTRACT.— Seismic reflection work was carried out in the southwest of Ankara around Polatlı-Haymana region as part of "Haymana Oil Exploration Project" The project area is located in Polatlı Basin extending in NW-SE direction and covering Triassic to Quaternary sediments. Seismic reflection data were recorded along profiles of 426 kilometers located in the area by Ünalan's work (Ünalan et al., 1979) in which the stratigraphy of the Upper Cretaceous-Lower Tertiary are described in detail. The upper boundary of Beyobası formation is the best reflector level in the data. This Maestrichtian Formation has been considered as the reservoir formation because of its fossileferous sandstone and limestone content. The contour map of the Beyobası formation was prepared and interpreted. The transition bands in the stratigraphic layers are generally not identified sufficiently. As the result of interpretation a NW-SE directional fault zone and two highs at both sides of this zone in the east part of the project area were obtained. The highs in the north and south of this zone are considered as parts of Kızılcakışla and Eski Polatlı anticlines. However, the north closing of the high located in the north and the south closing of the high located in the south could not be seen in the seismic data. In the west part of the project area two synclines were observed. The closing of one which is placed in the south is observable and the closing of the other one located in the north is not clearly observable.

INTRODUCTION

Seismic reflection work was carried out by General Directorate of Mineral Research and Exploration of Turkey (MTA), as part of "Haymana Oil Exploration" project in order to characterize the seismic stratigraphy in the field on the southwest of Ankara including Temelli, Polatlı, Haymana and Yenice regions (Fig. 1, 3).

The basement of the stratigraphic accumulation in the surveyed field was not described satisfactorily, however; the stratigraphic form of the Beyobası formation considered as a reservoir unit was defined and its upper boundary was contoured (Fig. 3).

GENERAL GEOLOGY

The detailed; stratigraphic study in the NW-SE directional Haymana-Polatlı basin was done by Ünalan (Ünalan et al., 1979). According to their study, the Upper Cretaceous-Lower Tertiary sediments a good prospect for oil are placed above Dereköy formation composed of serpentinitic limestone, radiolarit and volcanic blocks; which intern is underlain by Mollaresul formation of Upper Jurassic-Lower Cretaceous age lying discordantly over Temirözü formation consisting grey, wackes and meta-greywackes including Permian limestones pebbles.

The thickness of the Upper Cretaceous-Lower Tertiary sediment is 5800 meters. The Haymana flysch formation occure as a result of invasion of the Maestrichtian sea over the land and has a thickness of 1850 meters in block-section, Beyobası formation consisting of sandstone with fossiliferous limestone has a thickness of 125 meters in the block-section. These two formations cover the basement reflections mentioned previously. These formations are followed by Kartal, Çaldağ and Yeşilyurt formations deposited during lower Paleocene.
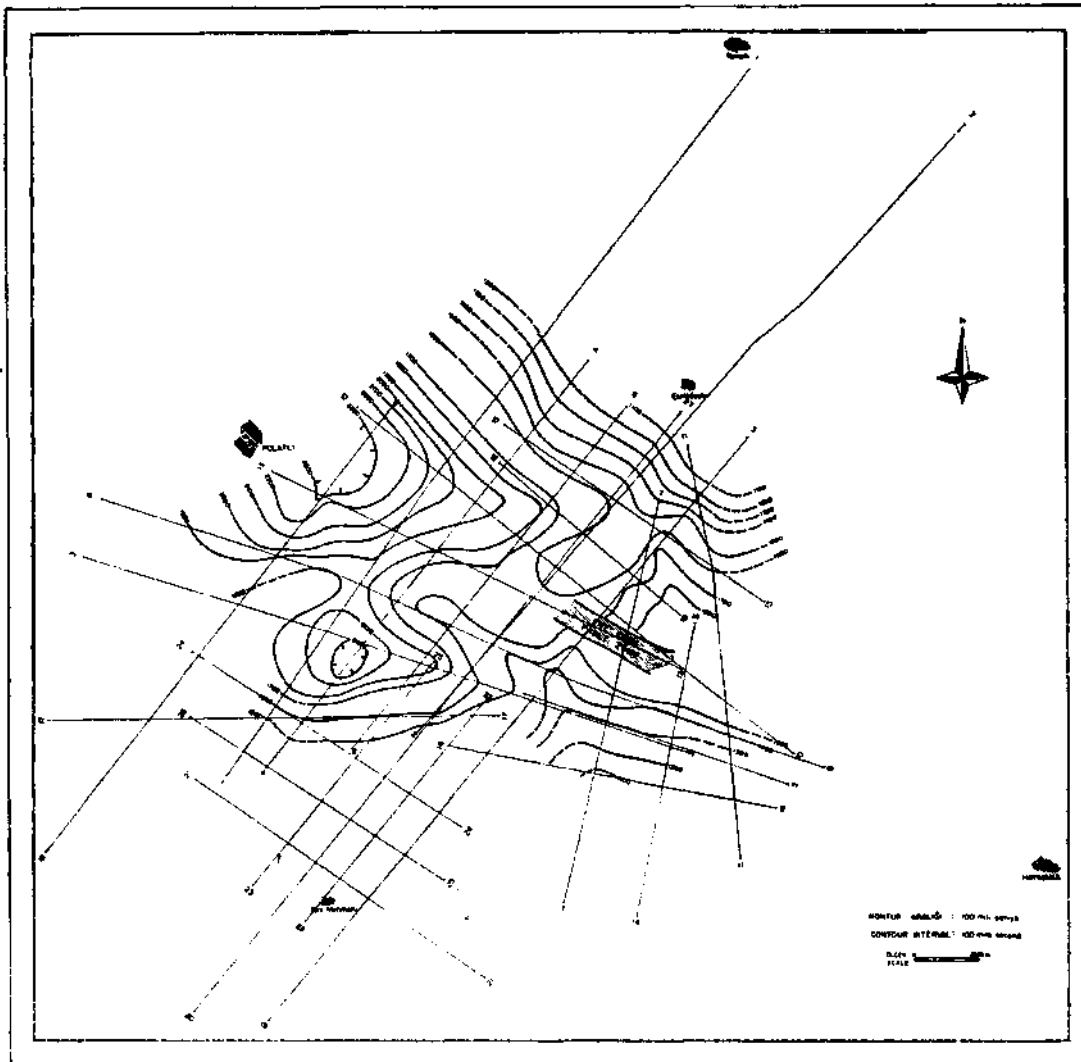
Fig. 1 – Geological map of the Haymana-Polatlı area (G. Ünalan et al., 1976).

Column headers:

SİSTEM (System)	SERİ (Series)	KAT (Stage)	FORMASYON (Formation)	SİMGE (Symbol)	KALINLIK-m (Thickness-m)	LİTOLOJİ (Lithology)
KUVA (Q)	Mio-Plio				0-200	Aluvyon (Alluvium) Çakıltaşı, marn, gölsel kçt., volkanik (Conglomerate, marl, lacustrine limestone, volcanics)
TERSİYER (Tertiary)	EOSEN (Eocene)	KÜZİYEN-LÜTESİYEN (Cuisian -Lutetian)	BELDEDE-DİÇAYRAZ-oYAMAK	Tya / Tça - Tb	525-1034	a)Kırmızı renkli çakıltaşı, kumtaşı marn (Red conglomerate, sandstone, marl) b)Sarı, bej, kumlu kçt ve marn (yellow, buff sandy clayey limestone and marl) c)Boz renkli çakıltaşı, kumtaşı, marn. (Grey conglomerate, sandstone, marl)
		İLERDİYEN (Ilerdian)	ESKİPOLATLI	Te	0-567	Boz renkli kumtaşı, marn, üste doğru kçt bantlı. (Grey sandstone, marl limestone banded upwards)
	PALEOSEN (Paleocene)		ILGINLIKDERE	Tı	40-350	Boz renkli çakıltaşı, kumtaşı (Grey conglomerate, sandstone)
		TANESİYEN (Thanetian)	KIRKKAVAK	Tkı	280-640	Algli kireçtaşı, boz marn (Algal limestone, grey marl)
		MONSİYEN (Montian)	KARTAL - ÇALDAĞ - ÇIYEŞİLYURT	Ty - Tç - Tk	0-1363	a)Kırmızı renkli çakıltaşı, kumtaşı marn (Red conglomerate, sandstone, marl) b)Algli kireçtaşı (Algal limestone) c)Kireçtaşı bloklu marn (Marl with limestone blocks)
KRETASE (Cretaceous)	ÜST KRETASE (Upper Cretaceous)	MAESTRİHTİYEN (Maestrichtian)	BEYOBASI	Kb		a)Kumtaşı, çakıltaşı (Sandstone, conglomerate) b)Boz renkli, çakıltaşı, mercekse1 kumtaşı içeren şeyl (Grey shale with conglomerate and sandstone lenses)
			HAYMANA	Kh	0-1842	
			DEREKÖY	Kd	0-415	Ofiyolit, kireçtaşı, radyolarit, volkanik (Ophiolites, limestone, radiolarite volkanics)
TRİYAS - JURA (Triassic - Jurassic)			TEMİRÖZÜ MOLLARESUL	JKm		Bej renkli yer yer masif kireçtaşı (Buff, locally massive limestone)
				Tjt		Kireçtaşı bloklu meta-grovak (Limestone blocky meta-greywacke)

Fig. 2- Generalized columnar section of the Haymana - Polatlı area (G. Ünalan et al. 1976).

Fig. 3 - Time countour map of Beyobası formation.

The Kartal formation which has 1362 meters thickness was formed with red terrestrial fragments deposited in the margin of the basin and it passes laterally to the Çaldağ formation in the basin direction, Çaldağ formation originates with algae limestone and enters laterally in the basin direction to Yeşilyurt formation which is turbidity limestone facies and has a thickness of 945 meters.

In the Middle Paleocene Kırkkavak formation composed of fossiliferous limestone with thickness of 640 meters in the block-section takes its place in the series and is overlain by Ilgınlıkdere formation (350 m) in flysch facies and Eski Polatlı formation (562 m) composed of sandstones with marl and gray mudstones. Beldede formation, consisting of conglomerate, marl and sandstone is placed at the top, of these series and is covered by Neogene continental sediments concordantly.

It has been concluded from the interpretation of the facies studies that there has been a shelf around Haymana, a shelf back in the north, west and south and a shelf front on the southwest of this area. It is also believed that during the Upper Cfetaceous and Lower Tertiary deposition period the Haymana-Polatlı basin emerged with salt lake towards south and made a connection with it and there has been a flysch deposition (Arıkan, 1975). That occurrence is interpreted as emergence of northern and western parts of the region as a result of being filled by sediments.

DATA ACQUISITION AND PROCESSING

The data acquisition has been done by using split-spread geophone arrengement along the lines total of 426 kilometers long. The data were recorded along these lines by using TI DFS IV recording instrument at 12 fold CDP coverege and are processed at the processing center of MTA by using TIMAP data processor.

Standart normal move out (NMO), constant velocity stack, TV filtering and spike deconvolution have been applied to the data in the processing steps.

The resolution of the data obtained in the middle and on the north side of the project area is good enough for the interpratation, but it is not good in the data obtained on the east, south and southwest sides of the project area as seen on the time-contour map (Fig. 3).

The information obtained from the well, drilled around Eski Polatlı, of 3500 meters depth (Özbudak and Yılmaz, 1980) and velocity determination studied in this well (Eres, 1978) were utilized in the interpretation stage.

SEISMIC LEVELS

The seismic levels are described below based on stratigraphic correlations as basement reflections, Cretaceous reflections, Eosen reflections and Neogen reflections.

The best seismic reflections correlated in all cross-sections were recorded from Beyobası formations and belongs to Cretaceous reflections. Other reflections decribed are not all continuous and can only be seen on certain seismic sections, in some cases they may be poor quality reflections. Description of seismic levels are as follows:

Basement reflections

No reflection level was accepted and correlated as a basement reflection in the whole cross-sections. However; some of the strong reflections groups, diveded by faults and suffered of diffractions beneath 2500 m. sec., have been considered as basement reflections. It is possible to correlate the basement with limestone of Upper Jurassic-Lower Cretaceous.

Cretaceous reflections

The seismic reflections correlated in all cross-sections were recorded from the top of the Beyobası formation. The velocity of the Beyobası formation, considered as a resorvoir formation, (5400 m. sec.) is the same as the velocity obtained for limestone and sandstone in the velocity determination studied in the well drilled in the working area (Eres, 1978).

The velocity of limestone placed at the top of the sequence (about 7000 m. sec.) is greater than that of Kartal formation (5057 m. sec.) as can be seen from sonic log. For this reason, the upper boundary of the Beyobası formation was obtained satisfactorily and time-contour map could be prepared (Fig. 3).

The reflections between the Beyobası formation and Haymana formation underlying under it are not clear because of a transition zone between them. The upper boundary of the Beyobası formation show an ondulation and is divided by faults as it is seen in the cross-sections (Fig. 4, 5, 6). It was concluded that the thickness of this formation does not change very much because the thickness of this formation is 174 meters in the well and is maximum 130 meters in the autcrops (Özbudak and Yılmaz, 1980). An additional work has been done in the south of the working area, in order to search the continuity of the Beyobası formation to the south (Fig. 3). However this was not possible as the quality of the data was not sufficient for the interpretation.

The reflections were seen time to time at the depth of seismic sections where the Haymana formation was to take place were considered as coming from consecutive layers of shale and sandstone (Fig. 4,5,6).

The upper boundary of the Kartal formation overlying the Beyobası formation concordantly has not been observed in some of the seismic sections since it was divided by faults and suffered by diffractions. However; it has been well observed between 180-390 CDP points of 2T line (Fig. 4).
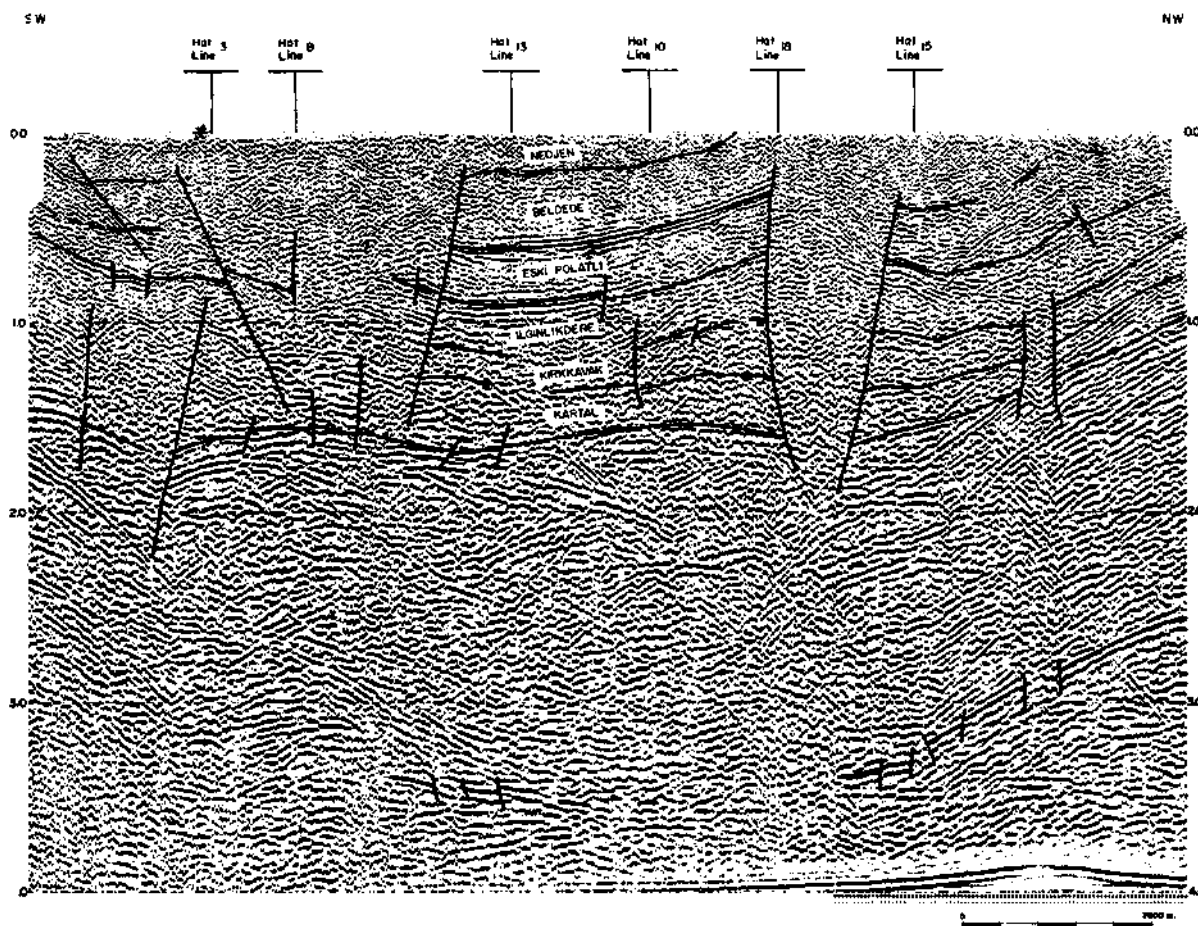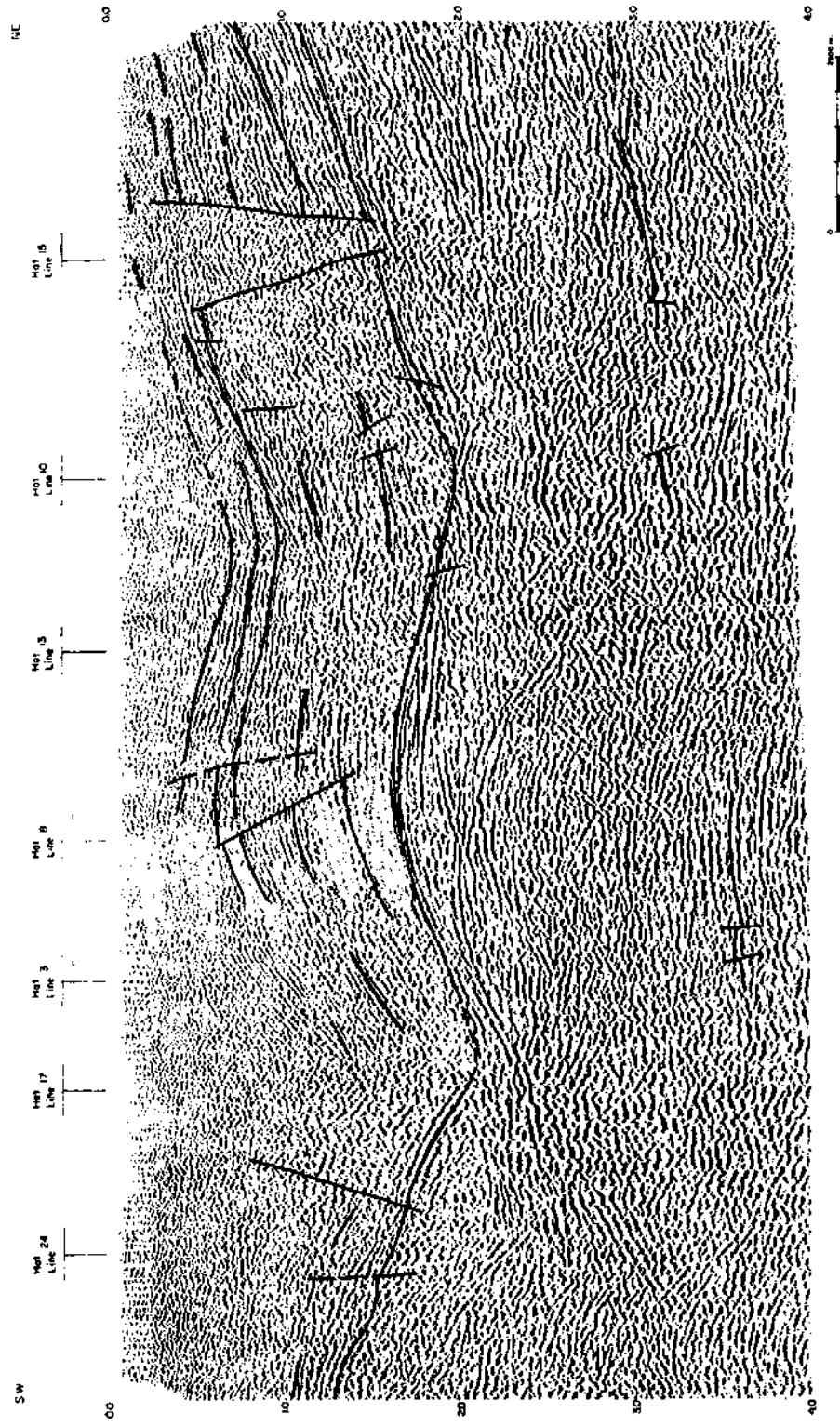

Fig. 4 - Interpretation of seismic line 2T.

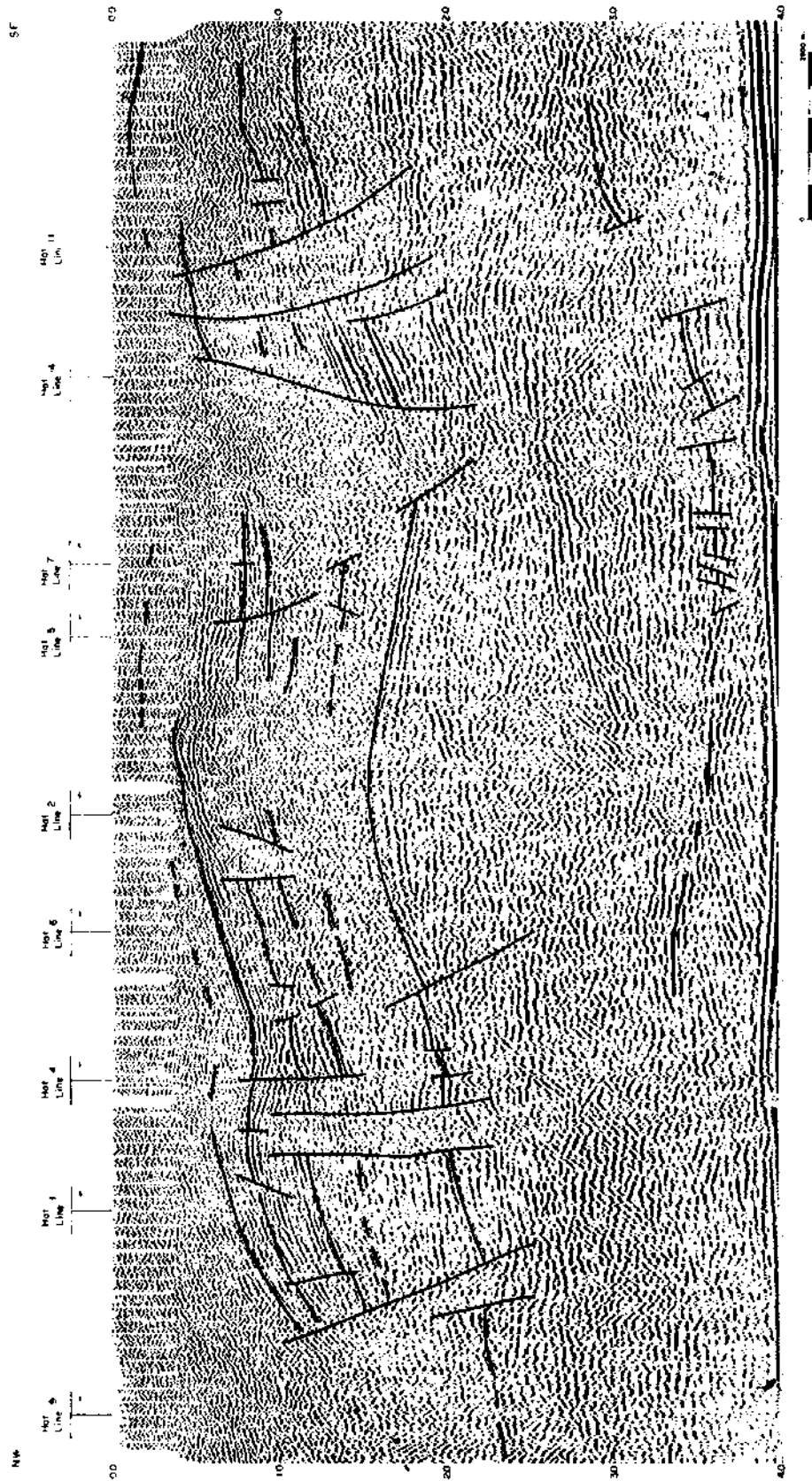**Fig. 5 – Interpretation of seismic line 4.**

Fig. 6 – Interpretation of seismic line 10.

The seismic reflections which could characterize the lateral transition zones of the Kartal, the Çaldağ and the Yeşildağ formations have not been observed clearly in the sections (Fig. 2).

Although the reflections from the lower boundary of the Kırkkavak formation overlying the Kartal formation are not observed clearly, it is possible to observe them between 240-400 CDP points of line 4 (Fig. 5).

The upper boundary of Ilgınlıkdere formation overlying Kırkkavak formation concordantly gives more prominent reflections (Fig. 4, 5, 6). These rather strong reflections were considered as coming from shale and sandstone bands.

Eosen reflection

Eski Polatlı and Beldede formations can be distinguished continually in some seismic sections like 4, 10, 27 (Fig. 4, 5, 6). These reflections have the some character with the Ilgınlıkdere reflections but they are more prominent than that of the Ilgınlıkdere reflections.

Neogen reflections

There is no prominent reflection to identify the Neogen formations with angular disconformitywith the formations beneath it (Fig. 5).

THE INTERPRETATION OF THE SEISMIC STUDY AND ITS GEOLOGIC RESULTS

The quality of the basement reflections is not good enough for the interpretation and does not allow their correlation in the whole project area. However; the top of some reflection groups at 2400-3600 m. sec., as seen in the seismic sections 2T, 4, 10 lines (Fig. 4, 5, 6) have been accepted as seismic basement.

The seismic basement shows rise towards east in the seismic sections 2T and 4 (Fig. 4, 5) and towards southwest in the seismic section 10 (Fig. 6). No information could be obtained for the south part of the project area because of the poor quality data.

The Beyobası formation, considered as a reservoir formation for its fossilereous sandstone and limestone content, has been observed at most parts of the project area (Fig. 3). As it is seen on the time-contour map, the Beyobası formation is rising towards NW regularly. This rise can be thought to point out to the Kızılcakışla anticline having a strike from the east of Eskiköseler to the 300 th shot point of the line 10 (Fig. 3, 6).

The upper boundary of the Beyobası formation in this anticline takes place at about 1550 m. sec. around the intersection of lines 10, 2T, at 1000 m. sec. in the south of Eski Köseler and makes no closure (Fig. 3).

The rise further to the north can not be followed due to the poor quality of reflections and the absence of seismic lines at this part.

The fault zone located on the east side of this rise seperates the Kızılcakışla anticline from the Eski Polatlı anticline whose strike is in the northeast-northwest direction. The upper boundary of the Beyobası formation rises from 1600 m. sec. to 1100 m. sec. at the Eski Polatlı anticline, and is located in a syncline whose strike is in the east-west direction, in the southwest reaching to 2100 m. sec. with a closure as seen on the time-contour map (Fig. 3). This boundary reaches to 2400 m.see. in the syncline, located in the west-northwest of the working area without closure.

It is necessary to conduct additional seismic studies both for determining the structures mentioned above and for better interpreting the basin located in a very interesting geological setting.

Manuscript received June 28, 1985

REFERENCES

Arıkan, Y., 1975, The geology and Petroleum prospects of the Tuz Gölü basin: MTA Bull., 85,17-35, Ankara-Turkey.

Eres, K., 1978, Polatlı-I Kuyusunda hız tayini ile ilgili kuyu atışı raporu: MTA Rep. (unpublished), Ankara-Turkey.

Özbudak, N., ve Yılmaz, H., 1980, Kuyu bitirme raporu: MTA Rep. (unpublished), Ankara-Turkey.

Ünalan, G.; Yüksel, V.; Tekeli, T.; Gönenç ,O.; Seyirt. O. and Hüseyin, S., 1976, Haymana-Polatlı yöresinin (Güney-batı Ankara) Üst Kretase-Alt Tersiyer stratigrafisi ve paleocoğrafik evrimi: Türkiye Jeol. Kur. Bull., 19, 159-176, Ankara-Turkey.

MIDDLE MIOCENE BIOSTRATIGRAPHY

Atike NAZİK** and Vedia TOKER***

ABSTRACT.— In this study, 21 planktonic Foraminifera species determined in the Middle Miocene sequence at the Karaisalı region of Adana. The following biozones in Langhian-Serravalian ages are distinguished: ? *Globorotalia fohsi lobata* zone, *Globorotalia fohsi fohsi* zone, *Globorotalia fohsi peripheroronda* zone. In addition to above mentioned planktonic Foraminifera, 13 Nannoplankton species are determined in the same samples. The result of this study has been compared with other studies which have been done in Trinidad, New Zeland, Libya, SW Africa and Nord Carrebean Sea and similar results are obtained. The fossil association and property of the sediments are also indicated that the environment is pelagic.

THE AGE AND LITHOSTRATIGRAPHIC CHARACTERISTICS OF KUMLUCA ZONE, ALAKIRÇAY GROUP; SW ANTALYA, TURKEY

Mustafa ŞENEL*

A sedimentary unit, described in the literature as Alakırçay unit (Marcoux, 1977), Kumluca Zone (Robertson and Woodcock, 1981), Kumluca complex (Yılmaz, 1981) and Alakırçay group (Şenel et al., 1981) is exposed in a N-S trending area of 30 km x 4 km at SW of Antalya and N of Kumluca. The unit consists of sandstone with plant fragments, conglomerate, siltstone, claystone, limestone with Halobia and chert nodules and bedded cherts, and is of Triassic age according to Marcoux (1977), but a Ladinian-Norian age is given to it by Şenel et al. (1981).
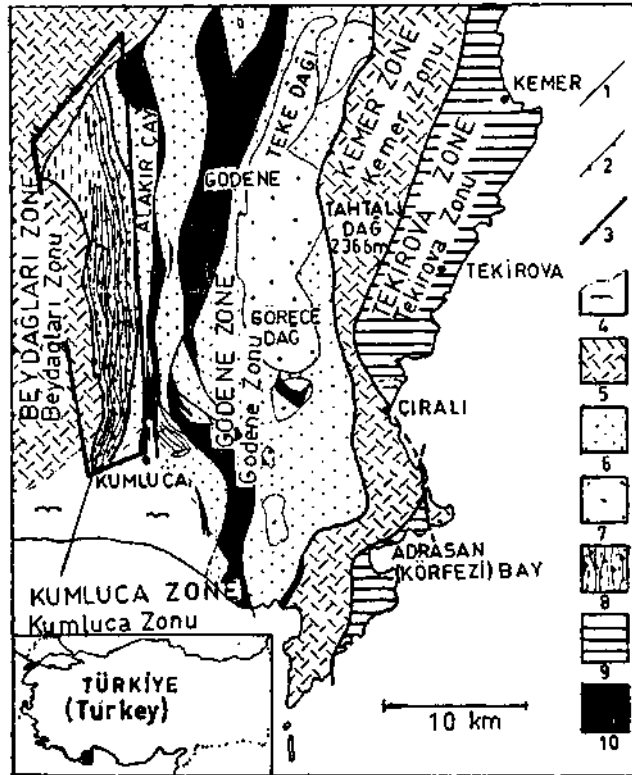

Fig. 1 - Location and geologic map (from Robertson and Woodcock, 1981). 1 - Stratigraphic contact; 2 - Thrust contact; 3 - Steeply dipping tectonic contact; 4 - Alluvium; 5 - Sediment on Pre-Triassic continental basement; 6 - Triassic mafic extrusives, thin sediment cover; 7 - Carbonate build-ups on salic Triassic mafic basement; 8 - Allochthonous sedimentary sequences in thrust sheets; 9 - Partial ophiolite sequence; 10 - Serpentinite.

Robertson and Woodcock (1981) have divided their Kumluca zone to three formations; Hatip and Bozyer formations of Upper Triassic and Karabük formation of Jurassic-Cretaceous. The Hatip formation has a transitional boundary with the overlying Bozyer and consists of interbedded sandstone with plant fragments, conglomerate, siltstone and claystone. The Bozyer formation is comprised of Halobia, Radiolaria and chert nodules containing micritic limestone and also has a transitional boundary with the Karabük formation which is represented by bedded cherts. Yılmaz (1981), has described the same unit (although she has called it Kumluca complex) as a sedimentary succession having shale, siltstone and sandstone with plant fragments at the base and limestone with Halobia, reef masses in marl and bedded chert succeding each other in the upper part of the unit. She has proposed the same age intervals as Robertson and Woodcock (1981).
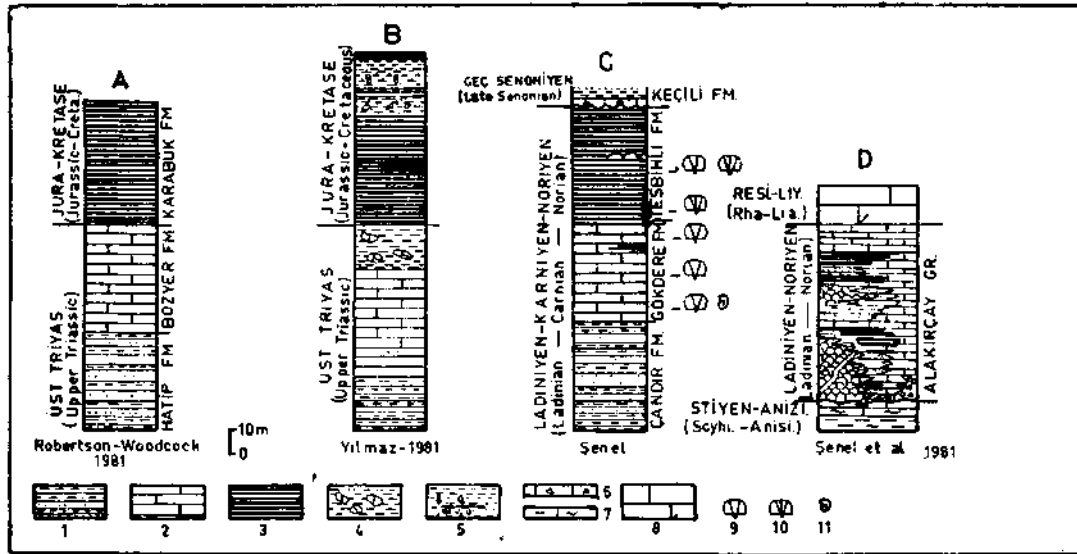

Fig. 2 - Generalized columnar sections. A-Kumluca zone; B - Kumluca complex; C - Columnar section of the Alakırçay group (vicinty of Karacaören) north of Kumluca; D - The generalized columnar section of the Alakırçay group.

1 - Claystone, siltstone, conglomerate, sandstone with plant fragments; 2 - Pelagic limestone; 3 - Bedded cherts; 4 - Reef masses, marl; 5 - Marl, claystone, siltstone, volcanogenic sandstone, mudstone, bituminous shale, redeposited calcarenite, calsirudite; 6 - Breccia; 7 - Vermicular facies; 8 - Neritic limestone; 9 - Halobia; 10 - Daonella; 11 - Ammonites.

During the investigation that is carried out by the author in the area N of Kumluca zone, contrary to the Yılmaz's (1981) finding no reef masses in marl is observed in between limestone with Halobia and bedded cherts. However these marls can be seen further to the N in areas around Dereköy, İmecik yayla, Bilalyeri and Çataltepe (Dereköy unit, Marcoux, 1977; Çataltepe unit, Poisson, 1977) and have no primary stratigraphic relation with the limestone with Halobias and belongs to a different tectonic unit.

Furthermore a zone containing Halobia and Daonella was found a few m (5-6 m) above the limestone and chert transitional boundary in addition to a 10 cm thick Halobia containing lens in the middle of the bedded chert layers indicating a Middle-Upper Triassic age, rather than Jurassic-Cretaceous as previously proposed.

The unit which was described under number of different names in previous studies (see above), is thought to be the lateral extent of the Alakırçay group which is widely distributed on the W and N of Antalya Bay (Alakırçay unit of Marcoux, 1977, and Ispartaçay formation of Poisson, 1977) and is of Middle-Upper Triassic (Ladinian-Carnian-Norian) age. As was stated in Şenel et al. (1981) the Alakırçay group is know to show rapid lateral and vertical lithofacies variations and claystone, siltstone, sandstone with plant fragments, limestone with Halobia, Radiolaria and chert nodules and bedded cherts are characteristic lithologies of Alakırçay group which also contain thin to thick pillow lavas in places.

The present nomenclature, i.e. Kumluca complex etc., is causing considerable confusion and thus should be abondened. Additionally, interpretations of the structural evolution of the region based on the assumption that bedded chert layers are Jurassic-Cretaceous in age, are bound to be wrong. Thus on the basis of these new findings it is proposed that the Middle-Upper Triassic bedded cherts ought to be included into the Alakırçay group.

Manuscript received November 11, 1985

REFERENCES

Marcoux, J., 1977, Geological sections of the Antalya region: Güvenç, T. and others, eds., Western Taurus excursion geological guidebook; VI. Colloquim on the geology of Aegean regions, Izmir.

Poisson, A., 1977, Recherches Geologiques dans les Taurides Occidentales (Turquie), These, L'Universite de Paris-Sud, Orsay, 795 pp.

Robertson, A.H.F. and Woodcock, N.H., 1981, Alakırçay Group, Antalya Complex, SW Turkey: A Deformed Mesozoic Margin: Sedimentary Geology, 30, 95-131.

Şenel, M.; Serdaroğlu, M.; Kengil, R.; Ünverdi, M. and Gözle, M.Z., 1981, Teke Torosları güneydoğusunun Jeolojisi: MTA Bull., 95/96, 13-43. Ankara-Turkey.

Yılmaz, P.O., 1981, Geology of the Antalya Complex, SW Turkey, (Ph. D. Dissertation): Austin, the University of Texas, University Microflims Inter., 268 p.